The Meteorological Magazine

April 1993

The unified model
Infrared imagery in record Atlantic low
Thunderstorms in a developing cyclone
World weather news — January 1993

The unified forecast/climate model

M.J.P. Cullen
Meteorological Office, Bracknell

Summary

The reasons for adopting a unified forecast/climate model are discussed. The model is described and related to previous forecast and climate models in use in the Meteorological Office. The software system used to implement it is also briefly described. Examples of its performance are shown in global, regional, and mesoscale forecasts, long-range forecasts, climate simulations, and upper-atmosphere forecasts.

1. Introduction

The Meteorological Office has used a global numerical weather prediction model since 1982 (Gadd 1985), and has used global climate simulation models since the late 1960s (Corby et al. 1977)). The global weather prediction model was based on the design of the then current climate model. Experience with the two separate models suggested that it would be advantageous to combine them at the next major computer upgrade. The opportunity occurred with the installation of the CRAY YMP in January 1990. It was also decided that the resulting unified model should be used for upper-atmosphere simulations taking advantage of the data supplied by the UARS satellite. This paper describes the justification for the move to a unified model, the model formulation and software system, and illustrates its performance in the main configurations.

2. Justification for the unified model

The global forecast and climate models implemented on the Meteorological Office CYBER 205 computer had many similarities. Both solved the equations of motion using finite difference methods on a grid regular in latitude and longitude. Both used a terrain-following vertical coordinate, with increased resolution near the ground and near the tropopause. Both included representations of the main physical processes such as boundary layer mixing, convection, large-scale precipitation, gravity wave drag, and radiation. The main differences were that lower horizontal and vertical resolutions were used in the climate model, that a different time integration scheme and arrangement of the variables on the grid were used in the two models, and that the representation of physical processes in the climate model was considerably more advanced. The program structure required for both models was similar. However, the climate model contained a large amount of ancillary software to enable output to be processed automatically during the very long integrations required.

State-of-the-art atmospheric modelling requires a high degree of scientific expertise, and it had already been necessary to share this expertise by using or attempting to use similar physical formulations in the two models. However, it is much simpler to do this if the models use the same computer code. Use of a modular program design allows easy testing of alternative formulations, and means that different representations of some processes can still be used if necessary. Either model on its own, together with ancillary programs for processing input and output data, forms a large software system. The unified model system contains at present about 150 000 lines of code. Maintenance of two separate systems is no longer practicable or justifiable. Furthermore, it had already

been decided that incorporating the output processing within the forecast model, as had already been done in the climate model, was a much more efficient method of generating the wide range of products required.

In order to achieve a unified model, however, several key steps had to be taken:
(a) Successful use in the climate model of the very efficient split-explicit integration scheme (Gadd 1978), used in the forecast model. This required modifying it to ensure conservation of heat and moisture, and ensuring acceptable performance in climate mode.
(b) Modifying the boundary layer scheme to allow use of the longer time-steps permitted by the split-explicit . integration scheme.
(c) Modifying the radiation and cloud scheme to allow use of the higher vertical resolution of the moisture field possible in the existing forecast model, and the planned unified model.
(d) Successful use in the forecast model of more-elaborate representations of physical processes, particularly the use of explicit cloud variables and their interaction with radiation.
(e) Design of a single maintainable software system to meet all the requirements, while achieving the same efficiency as a single-purpose model.

Following on from the initial operational implementation of the unified model, it was realized that there were considerable advantages in using the same model for the mesoscale forecast over the United Kingdom. This avoids the need to have two separate teams of scientists and two software systems, and allows the techniques used in larger-scale modelling to be rigorously tested at the higher resolution used in the mesoscale model against the detailed observations available over the United Kingdom. This experience, and the optimization of the model as a climate model, will also allow the model to be used with confidence as a relocatable limited area model anywhere in the world to meet defence requirements.

3. Description of the unified model

3.1 Equations of motion

The equations used are a more accurate approximation to the equations of motion than were used in the previous models. They are described in detail by White and Bromley (1988). They differ from those normally used in that the full three-dimensional representation of the of the Earth's rotation is included. This is necessary when planetary-scale motions are considered, and the vertical component of the Coriolis force may also be important in regions of strong vertical motion. In addition to the standard equations of motion, an arbitrary number of passive tracers can be advected by the model. This can be used to allow the model to study the evolution of chemical species, but could also be used to treat aerosols.

3.2 Grid and coordinate system

The equations are integrated in spherical polar coordinates, using a 'hybrid' vertical coordinate (Simmons and Burridge 1981). This is a function of pressure, equal to unity at the lower boundary, and equal to a multiple of pressure at the upper levels. It is chosen because terrain-following coordinate surfaces are much more convenient in the lower layers of the atmosphere, while pressure coordinates are more likely to give accurate results in the upper layers. The unified model code is designed to allow any distribution of levels. However, it is found in practice that the performance of physical parametrization schemes is very sensitive to the distribution of levels. Most users of the model will therefore be using the standard 19-level configuration shown in Fig. 1. The mesoscale model uses 30 levels, with extra levels between 25 metres above the ground and the tropopause. Upper atmosphere modelling will be using a 49-level configuration extending up to 0.25 hPa.

A regular latitude–longitude grid is used in the horizontal, with the variables arranged according to the Arakawa 'B' grid as in the operational 15-level model (Gadd 1985). The arrangement of variables in the vertical is also the same as in the 15-level model. The code can be run at any desired resolution, subject to computer memory restrictions. The operational forecast grid has spacing of $0.8550°$ in latitude and $1.250°$ in longitude. The standard climate and upper-atmosphere configurations will use $2.50°$ and $3.750°$.

The limited-area models also use spherical polar coordinates. However, to obtain uniform resolution over the area of interest, the coordinate pole is not placed at the geographical pole. This idea was first introduced in the Irish limited-area model (Unden 1980). The unified model can be run with any choice of coordinate pole and area. The operational regional model has the coordinate pole at 30 °N, 160 °E and a grid-length of 0.44°. The mesoscale model has the coordinate pole at 37.5 °N, 177.5 °E and a grid-length of 0.15°. The integration areas for the regional and mesoscale models are shown in Fig. 2.

3.3 Finite difference scheme

The split-explicit finite difference scheme used in the 15-level model is very efficient, and there was no need to change it for purely forecast applications. However, finite difference schemes for climate modelling have to satisfy additional requirements, for instance that total heat and moisture must be conserved under advection. To meet these requirements, the Lax–Wendroff advection scheme was replaced by the Heun scheme, and the separation of calculations between the long advection step and the short adjustment step had to be altered. The new scheme is described in detail by Cullen and Davies (1991). As with the 15-level model, Fourier filtering has to be used at high latitudes in the global model in order to prevent an undesirable restriction on the time-step that can be used. However, to ensure conservation, it is
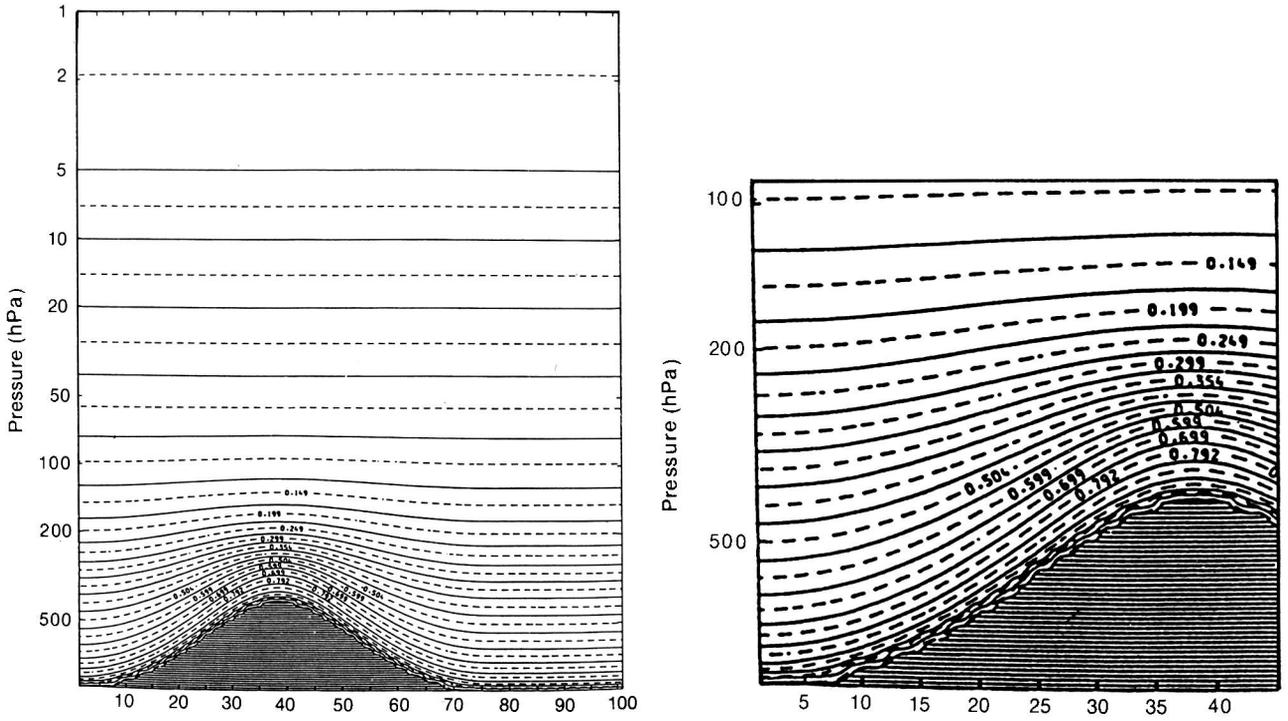
Figure 1.   Standard levels for use in the unified model.
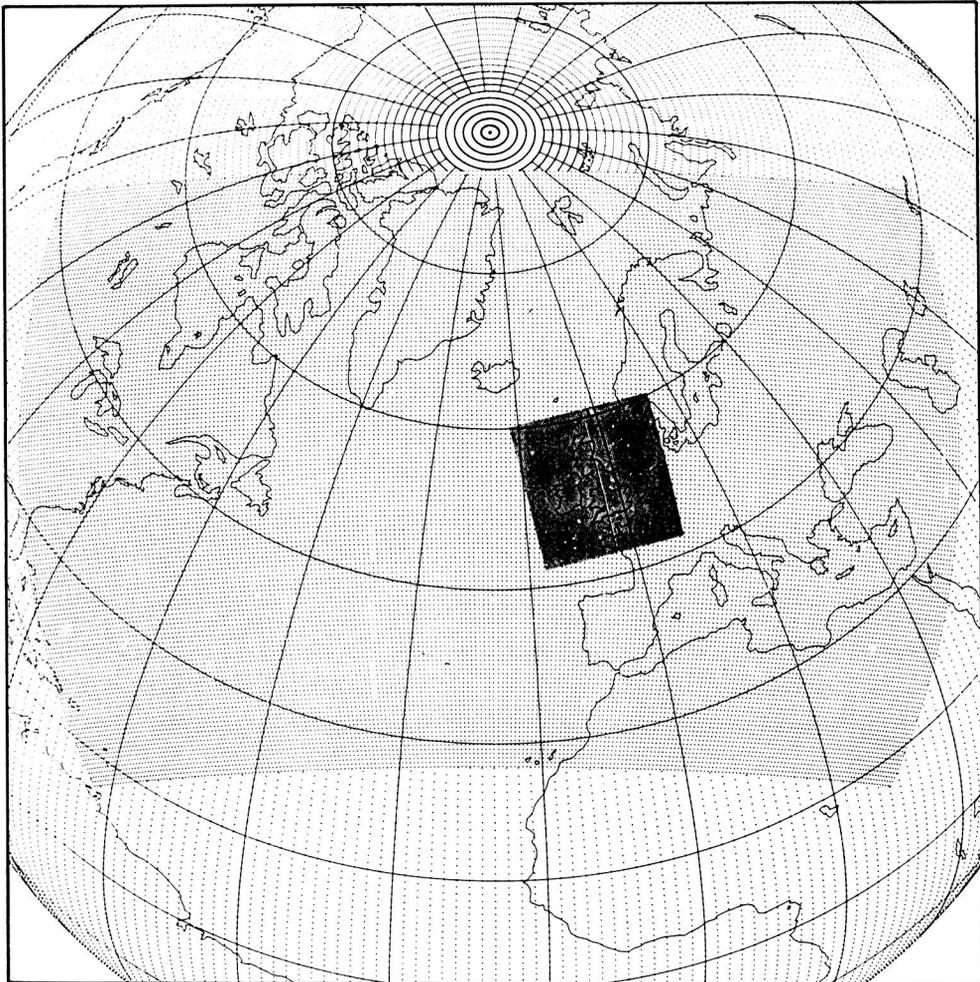

Figure 2.   Integration areas for the regional and mesoscale models.

necessary to filter increments to the temperature and moisture fields rather than to filter the fields themselves. No filtering is required in the limited area model.

3.4 Parametrizations

It is expected that a library of parametrizations will gradually become available for the unified model. Those that are being used initially are described briefly below.

(a) Land surface model. A multilayer soil temperature model and a soil moisture prediction scheme are included. Different soil types are specified, and used to determine the surface albedo. A model of the vegetation canopy is included. Moisture can be retained in the canopy or transferred to the soil or atmosphere. Different vegetation types can be specified. Snow depth is predicted and used in the calculation of albedo. The scheme is described in detail by Smith (1990) and Gregory and Smith (1990).

(b) Boundary layer. Vertical turbulent transport of primary variables and tracers in the boundary layer depends on the local Richardson number. The presence or absence of cloud is taken into account in calculating the transport coefficients. The scheme is described in Smith (1990).

(c) Large-scale cloud and precipitation. Large-scale clouds are represented by their liquid water (or ice) content. The total optical thickness of the clouds is taken into account in the radiation calculations (Ingram 1990). Large-scale precipitation is calculated in terms of the water or ice content of the cloud; frozen cloud starts precipitating as soon as it forms. Cooling of the atmosphere due to evaporation of precipitation is included. The scheme is described by Smith and Gregory (1990).

(d) Convection. Sub-grid-scale convective processes are modelled using a simple cloud model; convection affects the large-scale atmosphere through compensating subsidence, detrainment, and the evaporation of falling precipitation. The scheme is described and illustrated by Gregory (1990) and Gregory and Rowntree (1991).

(e) Radiation. The radiation calculation uses six bands in the long wave and four in the solar calculation. It allows for water vapour, ozone, carbon dioxide, and the large-scale and convective cloud distributions. Cloud radiative properties depend on cloud water and ice content. The scheme is described by Ingram (1990).

(f) Gravity-wave drag. The effects of the drag caused by sub-grid-scale gravity waves is estimated using the sub-grid variance of the orography and the known absorption properties of gravity waves in a given atmospheric profile. The scheme is described by Wilson and Swinbank (1991).

(g) Horizontal eddy diffusion. This is represented by simple grid-scale filters The filters can be iterated to make them more scale selective for use at low resolution. The method is described by Cullen *et al.* (1991).

(h) Vertical eddy diffusion. This is sometimes required to remove oscillations caused by inadequately resolved quasi-inertia waves. Only the winds are smoothed. The method is described by Wilson (1992).
(i) Ancillary fields. The calculations of surface exchanges require values of a number of surface parameters. Distributions of sea-ice and snow cover must be specified. Over the open sea, the surface contact temperature has to be analysed for forecast use. Over the land, sets of parameters defining the soil and vegetation characteristics must be specified.

3.5 Coupling to other models

Various types of coupling are available.
(a) Ocean model. The atmosphere model can be coupled to both global and limited-area ocean models. It can also be coupled to a highly simplified ocean model known as a 'slab' model. The unified model system can be used to run ocean-only integrations.
(b) Stratosphere-only model. The full atmosphere model can be used to generate the heights of an isobaric surface to drive a version of the unified model covering only the stratosphere.
(c) Limited-area models. The global atmosphere model drives the regional model by generating values of the prognostic variables in a boundary zone. When the regional model is integrated, the values on the boundary are constrained to be the same as those in the global model, with those close to the boundary replaced by a weighted mean of predicted values and prescribed values from the global model (Davies 1976). A similar method is used to drive the mesoscale model from the regional model.
(d) Wave model. This is driven by 10 m winds output from the atmosphere model. It is likely that in future the wave model will be coupled to the atmosphere model and used to predict the surface roughness over the sea.
(e) Surge model. This is driven by model surface pressure and wind output.

3.6 Software implementation

An overview of the unified model software system is shown in Fig. 3.

The main components are:
(a) User interface. A panel-driven system which allows a user to run any version of the model with any choice of diagnostic output. It holds a library of previous experiments conducted by the user, so that it is easy to make small changes to a previous experiment with the model.
(b) Reconfiguration. A system for converting an input unified model data set to a new resolution, importing new ancillary or analysed data, and expanding the data set to make room for extra diagnostics.
(c) Model. The atmosphere and/or ocean model is integrated with data assimilation if required.
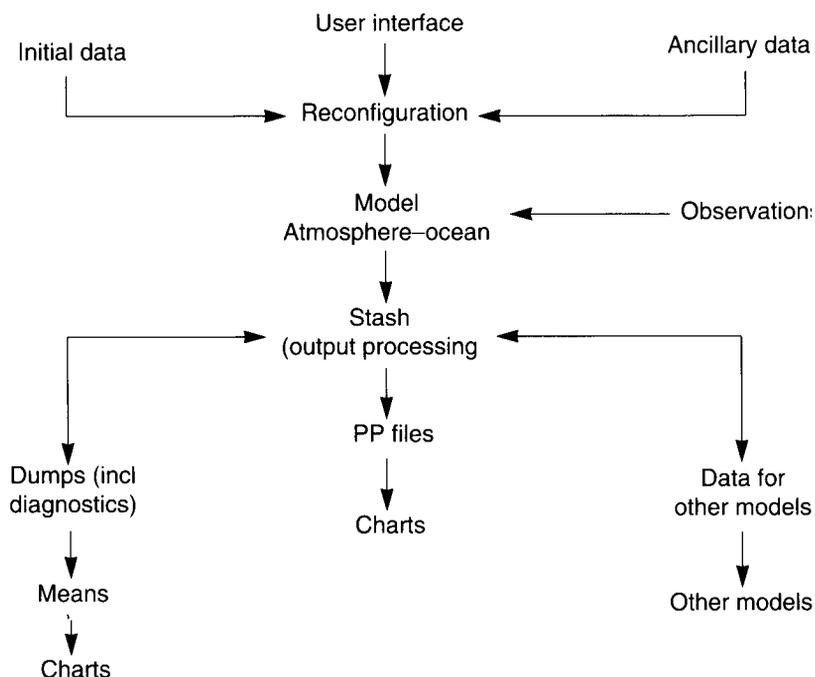
Figure 3. Unified model software system.

(d) Stash diagnostics. Diagnostics generated in each section of the model are processed as required by the user, either being output to the front-end computer or being retained for later time-averaging.

(e) Output streams. This includes the output for coupling to other models, dumps to allow integrations to be restarted, and chart output. Output can be time-meaned if required.

4. Examples of the use of the unified model.

4.1 Global forecasting

The enforcement of conservation properties in the integration scheme is the main dynamical difference between the unified model and the previous Meteorological Office forecast model. This appears to be the reason why the unified model is much better at predicting upper ridges. An example is shown in Figs 4–6. The ridge in the verification 500 hPa chart (Fig. 4) devel-- oped over the previous 4 days. Though the unified model slightly underestimates the amplitude, it is still 12 dam greater than that produced by the old forecast model. Other experiments showed that the resolution difference between the two models had only small effects on this type of development.

4.2 Regional forecast

The higher resolution and possibly the more advanced physical parametrizations of the operational limited-area version of the unified model allow it to give a more organized representation of regions of precipitation than the previous limited-area model. On occasions, the higher

resolution also gives a better treatment of pressure systems. An example is shown in Figs 7–9, where the depression to the east of Scotland is much better represented by the new model 24 hours ahead.

4.3 Mesoscale forecast

The initial version of the unified mesoscale model matches the previous mesoscale model in horizontal resolution, and vertical resolution above the near-surface layer. Further development is required to include the near-surface layers and allow useful fog predictions. It is hoped to complete this enhancement later in 1993. The initial version has proved successful in adding detail to precipitation forecasts from the regional model, while retaining greater consistency with it than did the previous mesoscale model. An example is shown in Figs 10–12. The new mesoscale model gives an equivalent amount of detail to the old model, in some respects better and in some worse when compared to the verifying radar picture.

4.4 Long-range forecasting

The standard long-range forecast procedure is to run a set of nine forecasts from data times six hours apart (Milton 1990). The results are then averaged over a set of forecast periods, including days 6–15 and days 16–30. An example of an exceptionally good forecast made from the average of forecasts from data times between 18 and 20 May 1991, verifying for the period 26 May to 4 June, is shown in Figs 13 and 14. The cool north-easterly flow over the United Kingdom is very well predicted. This forecast had an anomaly correlation coefficient of 0.79. The average value of this coefficient for unified model forecasts for this range to date is 0.17.
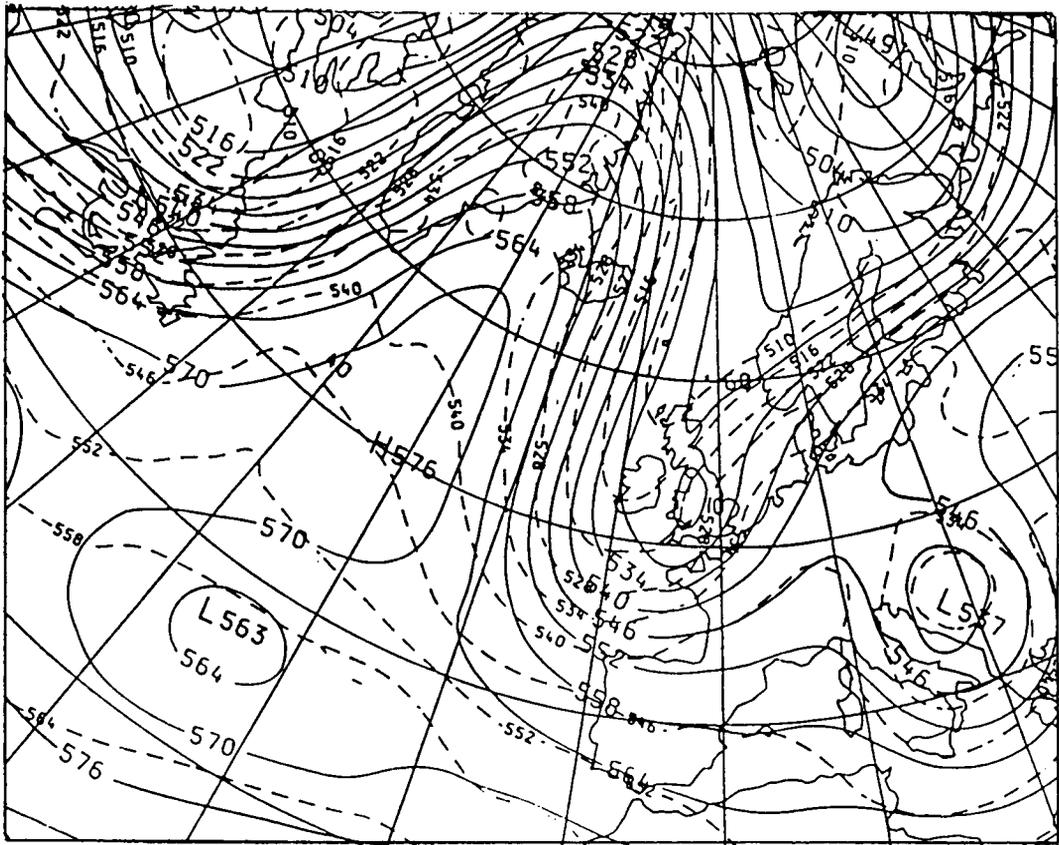
**Figure 4.** Analysis at 500 hPa for 00 UTC on 8 December 1990.
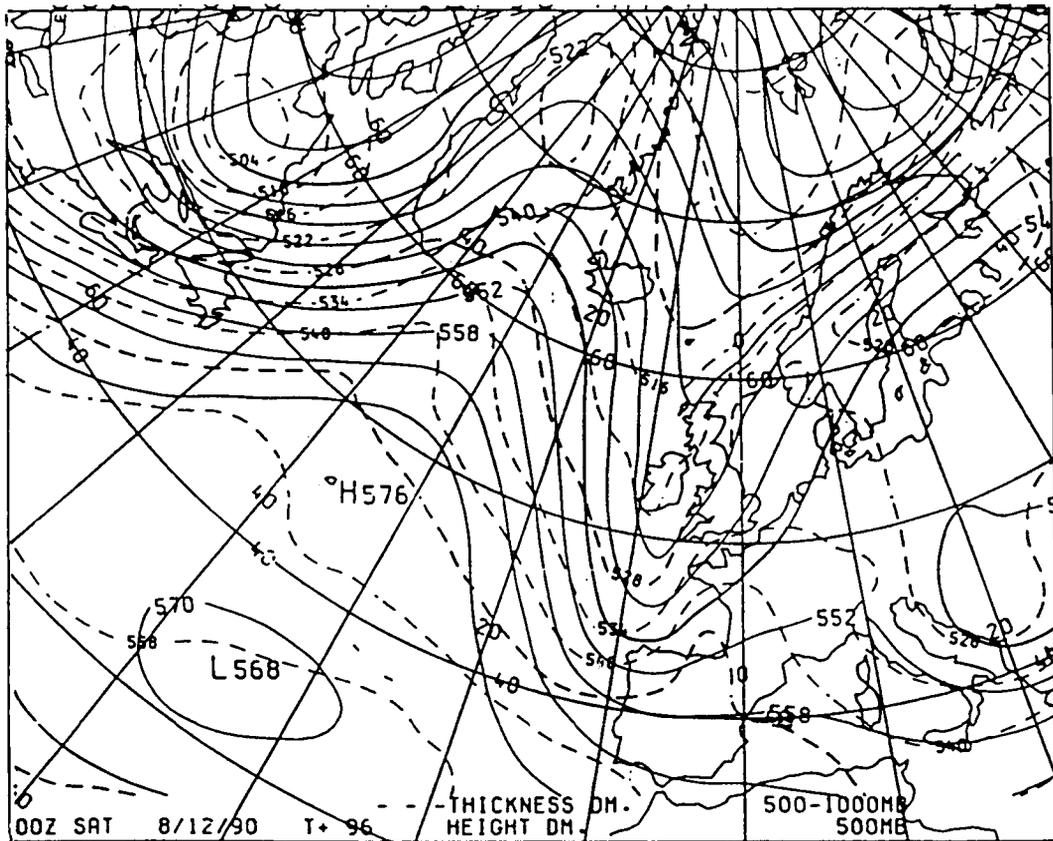
Figure 5. Four-day 500 hPa forecast valid at 00 UTC on 8 December 1990 using the previous Meteorological Office forecast model.
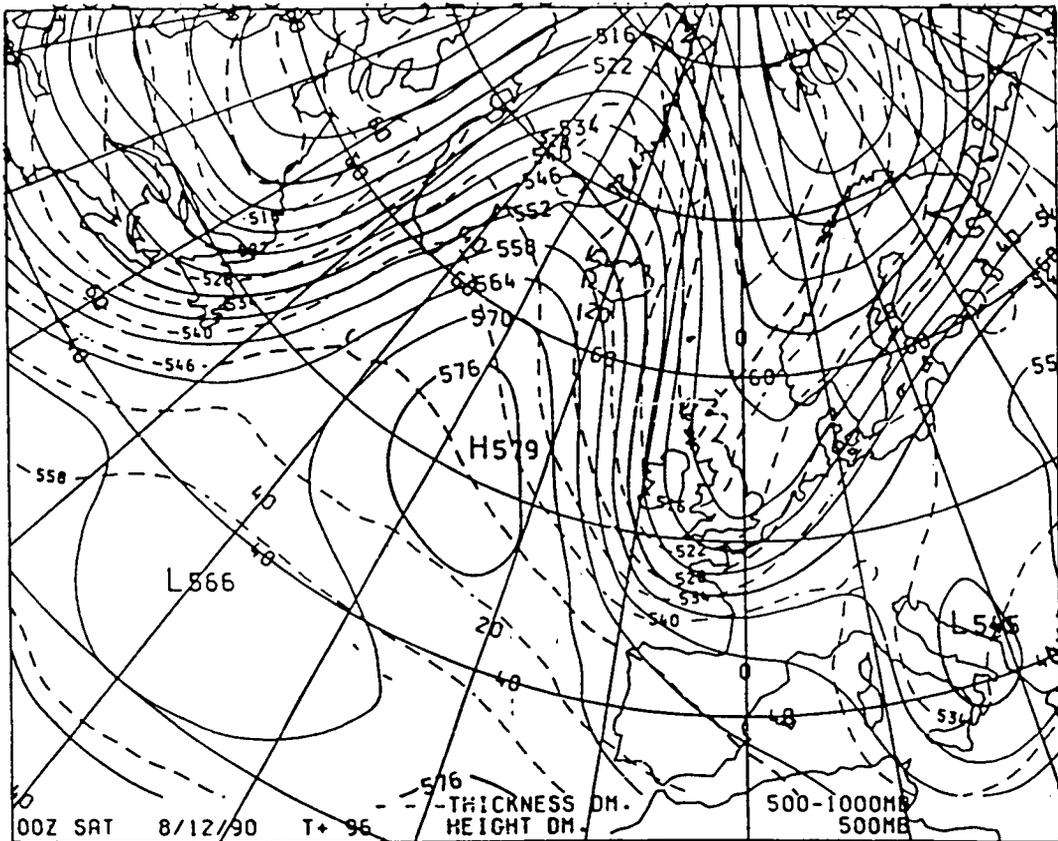
Figure 6. Four-day 500 hPa forecast valid at 00 UTC on 8 December 1990 using the unified model.
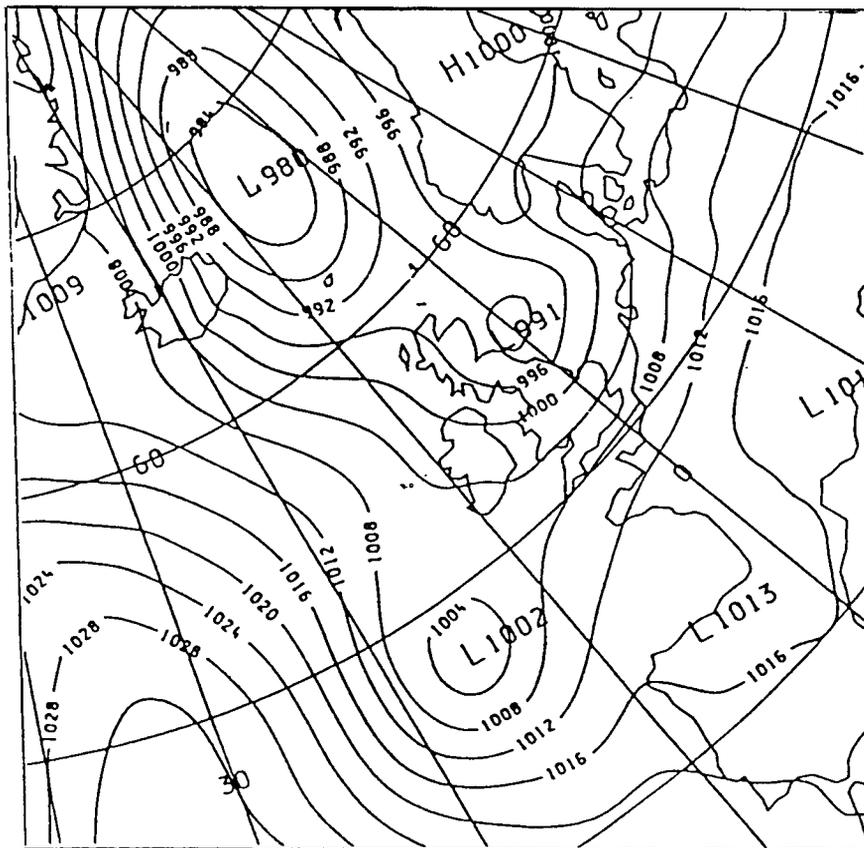

Figure 7. Surface pressure analysis (hPa) for 00 UTC on 21 March 1991.
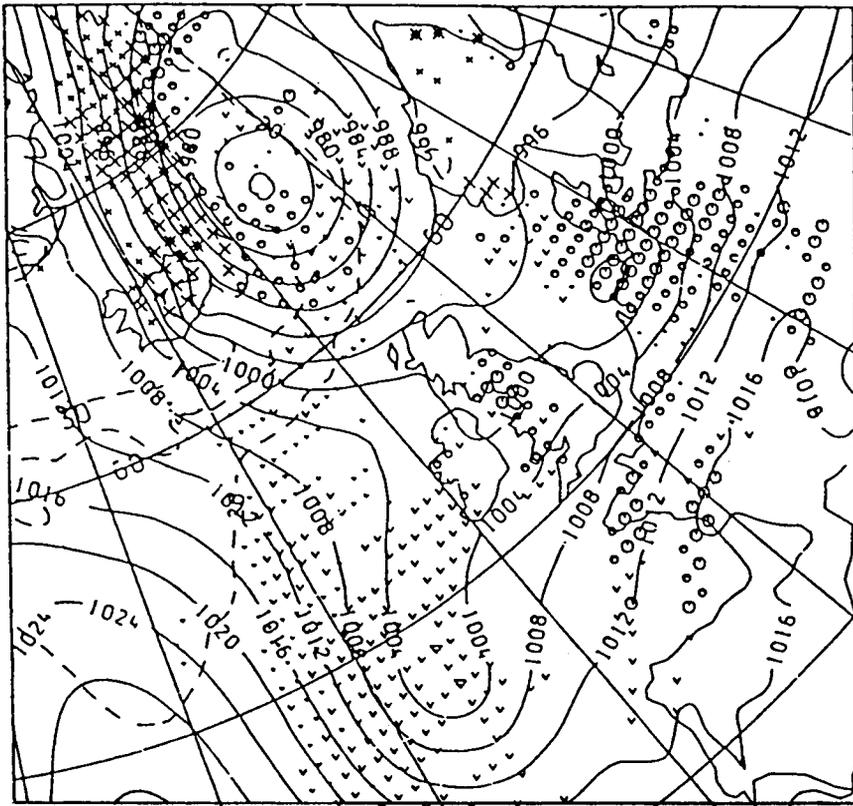
**Figure 8.** Twenty-four-hour mean-sea-level pressure forecast (hPa) for 00 UTC on 21 March 1991 using previous model.
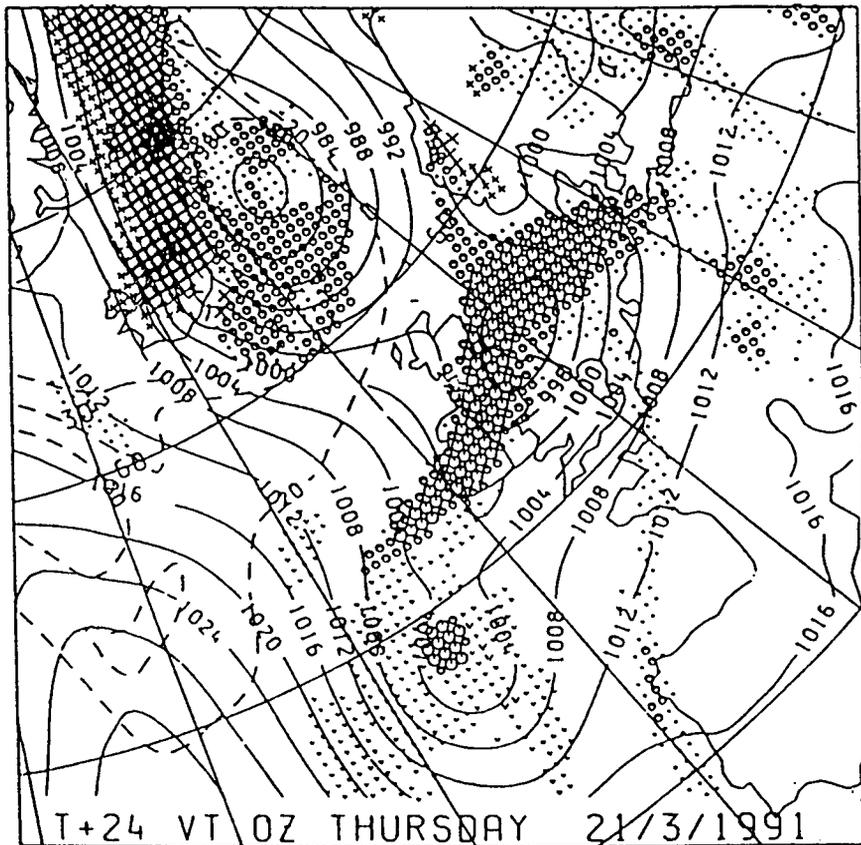
Figure 9. Twenty-four-hour mean-sea-level pressure forecast (hPa) for 00 UTC on 21 March 1991 using the unified model.
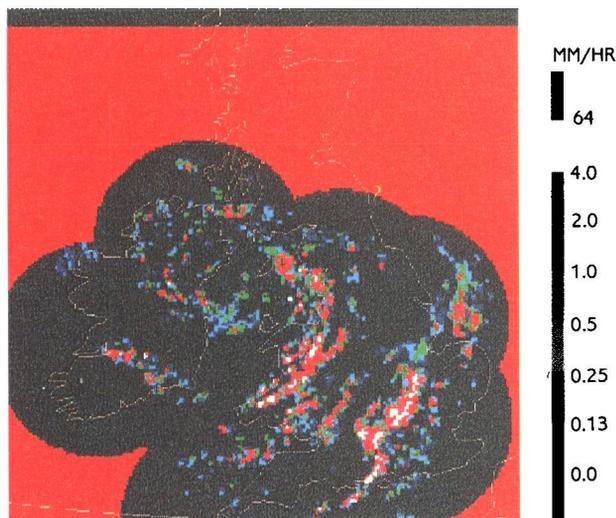
Figure 10. Weather radar network picture showing the observed rainfall distribution corresponding to the forecast in Figure 12.
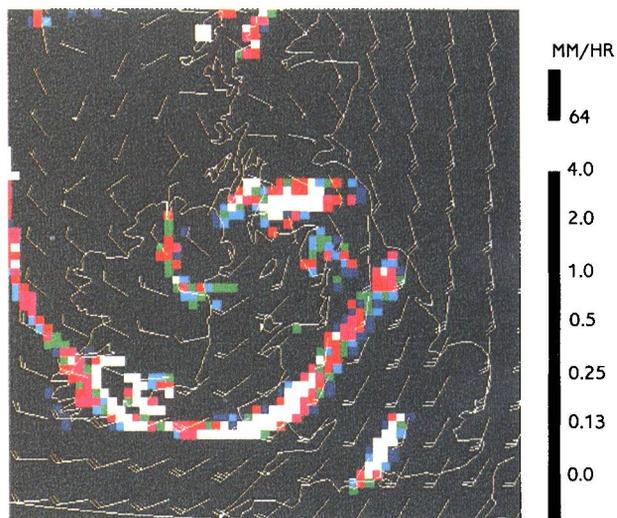
Figure 12. Twelve-hour forecast of rain bands from the Meteorological Office non-hydrostatic mesoscale model valid at 12 UTC on 23 August 1991.
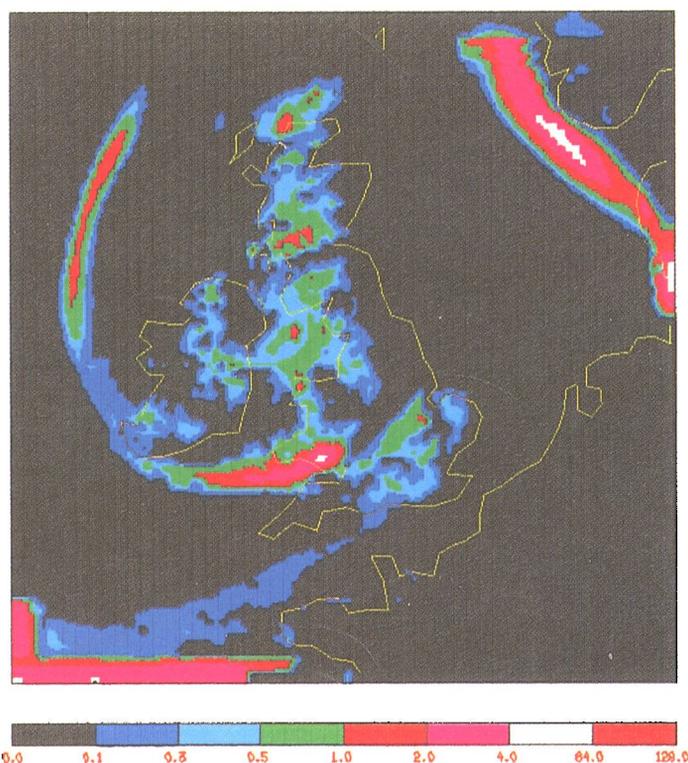
Figure 11. Twelve-hour forecast of rain bands from the mesoscale version of the unified model valid at 12 UTC on 23 August 1991.

4.5 Climate simulation.

Figs 15 to 17 show the rainfall climatology for the unified model for the northern hemisphere winter compared with climatology and the previous climate model. The unified model results are a 20-year mean, and the climatological estimate is that of Jaeger (1976). The simulations are broadly comparable. Comparisons over the full annual cycle show that the unified model gives lower monsoon precipitation over the Sahel and Venezuela when compared to climatology and the previous model. The unified model gives excessive summer precipitation over the South China Sea. The previous model gave an unrealistic zonal band of minimum precipitation along the equator in the west Pacific and Indian ocean, which is not present in the unified model.
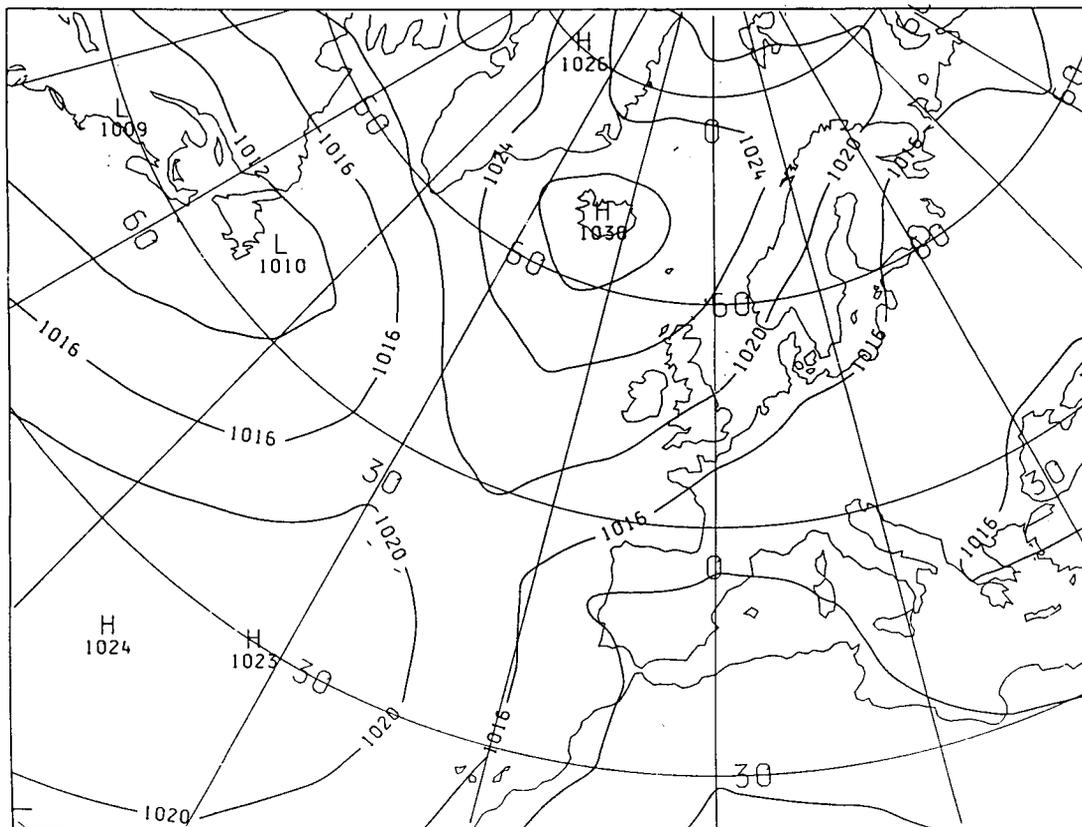
Figure 13. Ensemble mean of 9 unified model forecasts of the average mean-sea-level pressure (hPa) from 00 UTC on 26 May 1991 to 00 UTC on 4 June 1991.
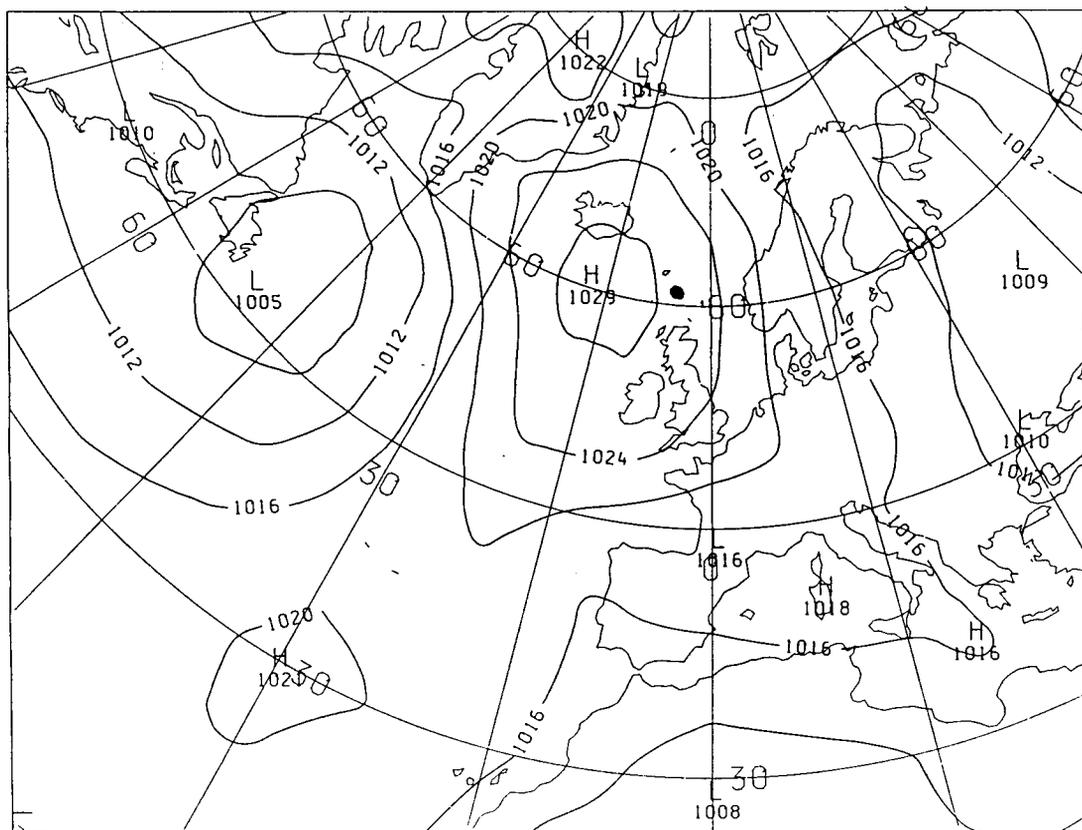
Figure 14. Ten-day mean of mean-sea-level pressure (hPa) from 00 UTC on 26 May 1991 to 00 UTC on 4 June 1991.
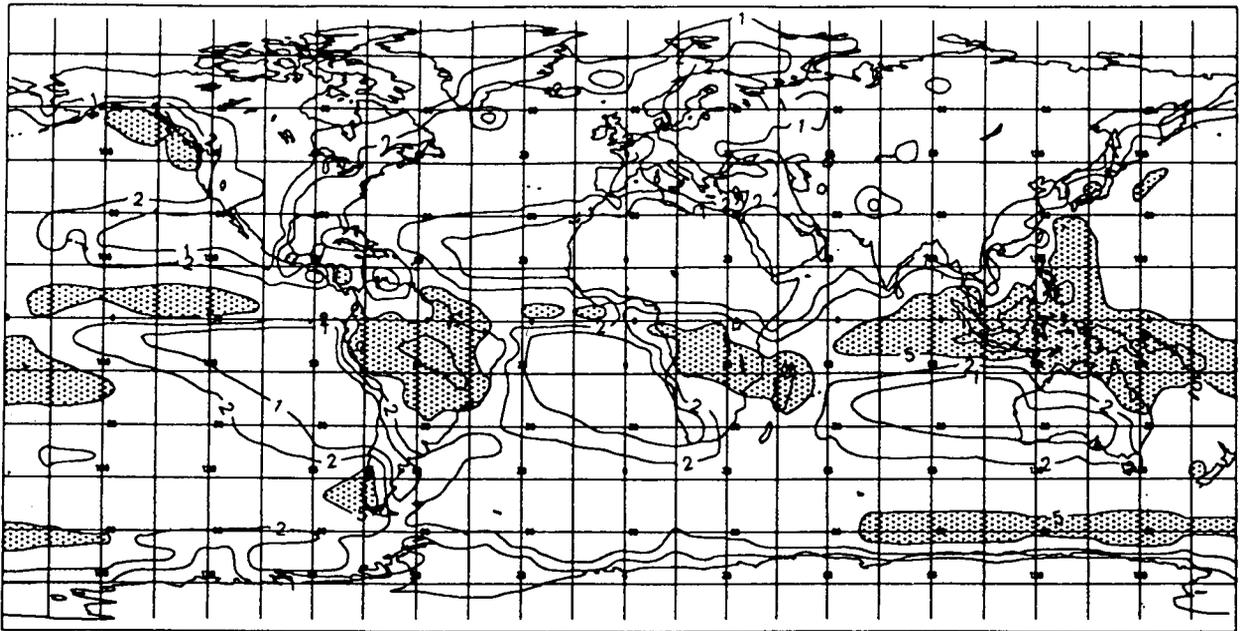
**Figure 15.** Climatological precipitation estimates (Jaeger) with contours at 1, 2, 5, 10, 20 and 40 mm d $^{-1}$. Areas over 5 mm d $^{-1}$ are shaded.
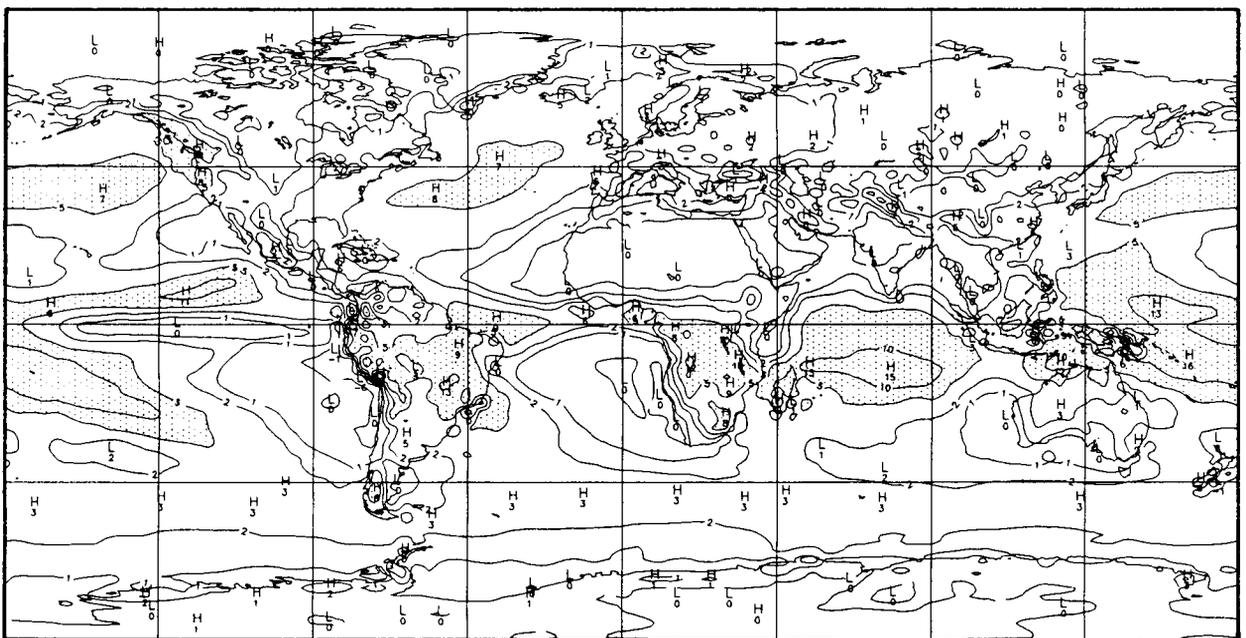
Figure 16. December–February precipitation (unified model) with contours at 1, 2, 5, 10, 20 and 40 mm d $^{-1}$ Areas over 5 mm d $^{-1}$ are shaded.

4.6 Upper-atmosphere forecasting

A 5-day forecast of a stratospheric warming event using a 42-level version of the model extending to 0.25 hPa is shown in Figs 18 and 19. The 10 hPa height is illustrated. At the initial data time, there was a single polar vortex at this level. The model has correctly forecast the splitting of the vortex into two, though it has produced two separate upper-high centres rather than the cross-polar ridge shown in the observations.

4.7 Coupled ocean–atmosphere forecast

The ocean component of the unified model has not been changed from the previous CYBER model. An example of the coupled model capability of the unified model is shown in Fig. 20. This shows the 5-year mean sea surface temperature anomaly relative to climatology produced after an initial 25-year calibration period.
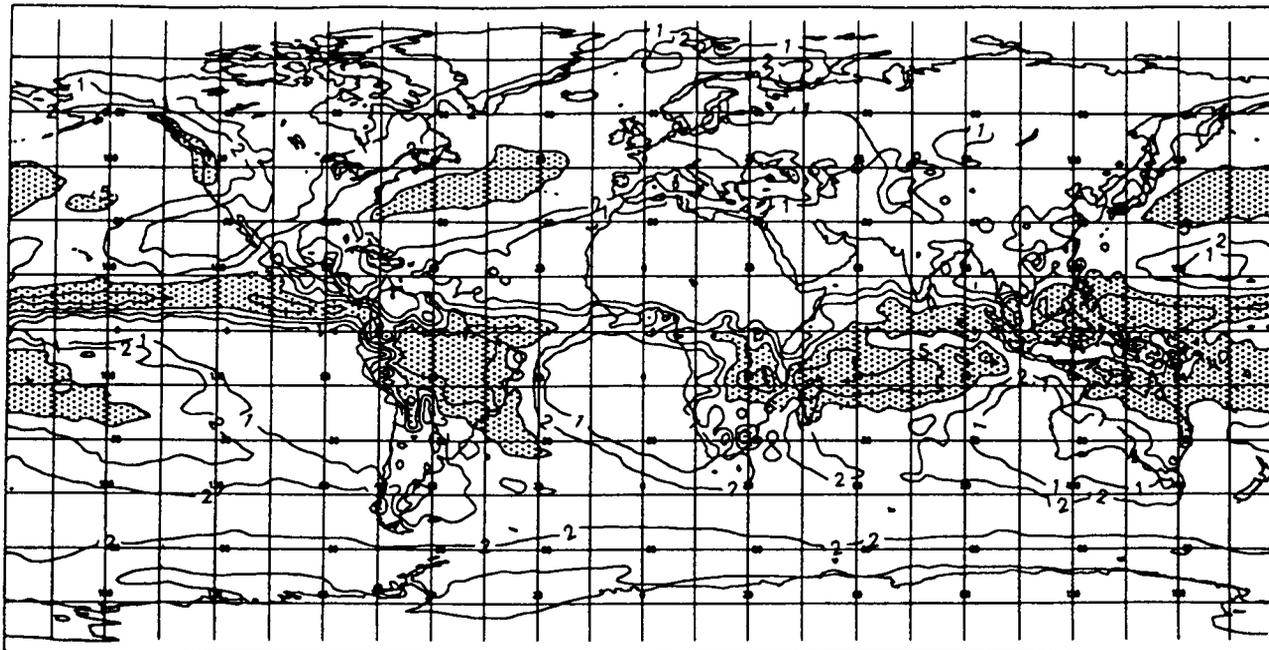
Figure 17. December–February precipitation (previous climate model) with contours at 1, 2, 5, 10, 20 and 40 mm d^{-1}. Areas over 5 mm d^{-1} are shaded.
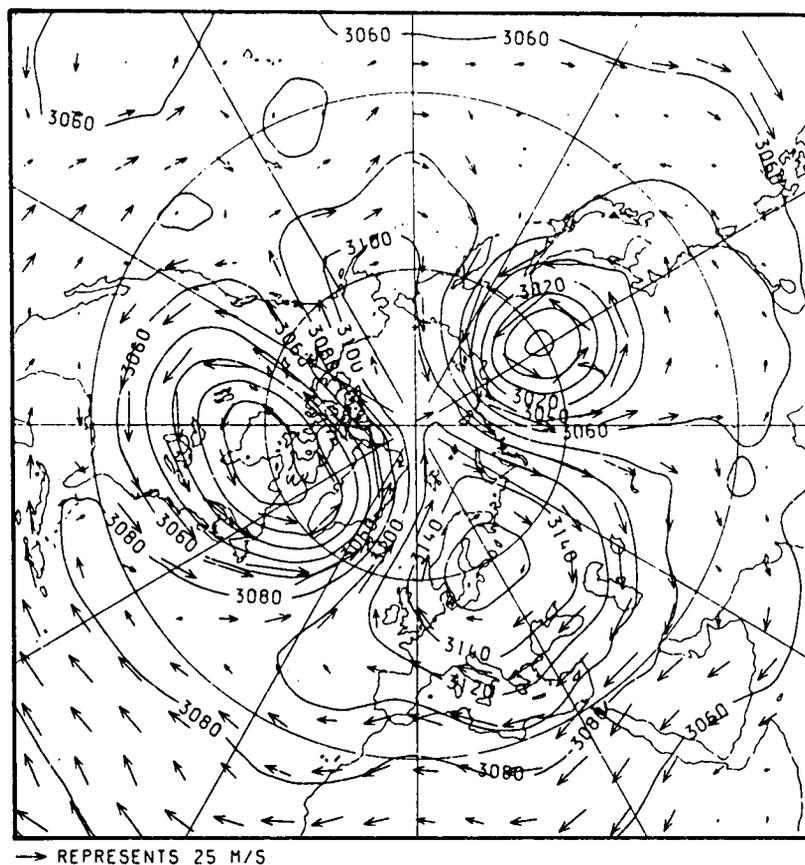
Figure 18. Height (dam) and wind analysis at 10 hPa for 12 UTC on 20 February 1989.
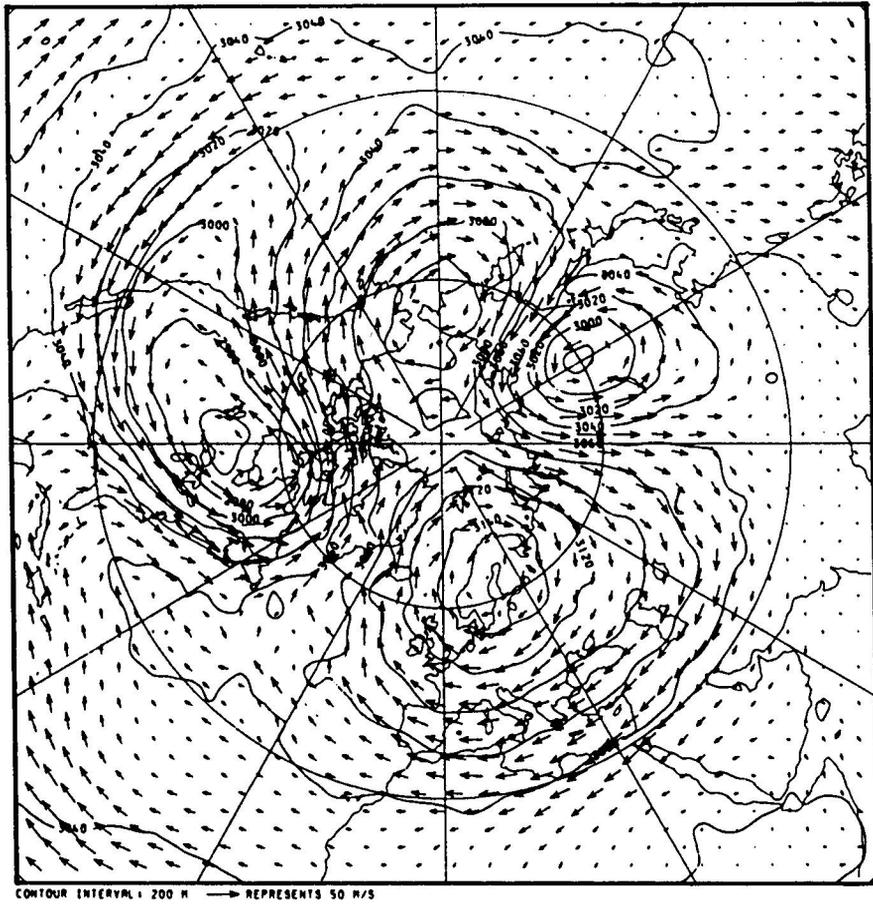
Figure 19. Five-day 10 hPa height (dam) and wind forecast valid at 12 UTC on 20 February 1989 using the 42-level version of the unified model.
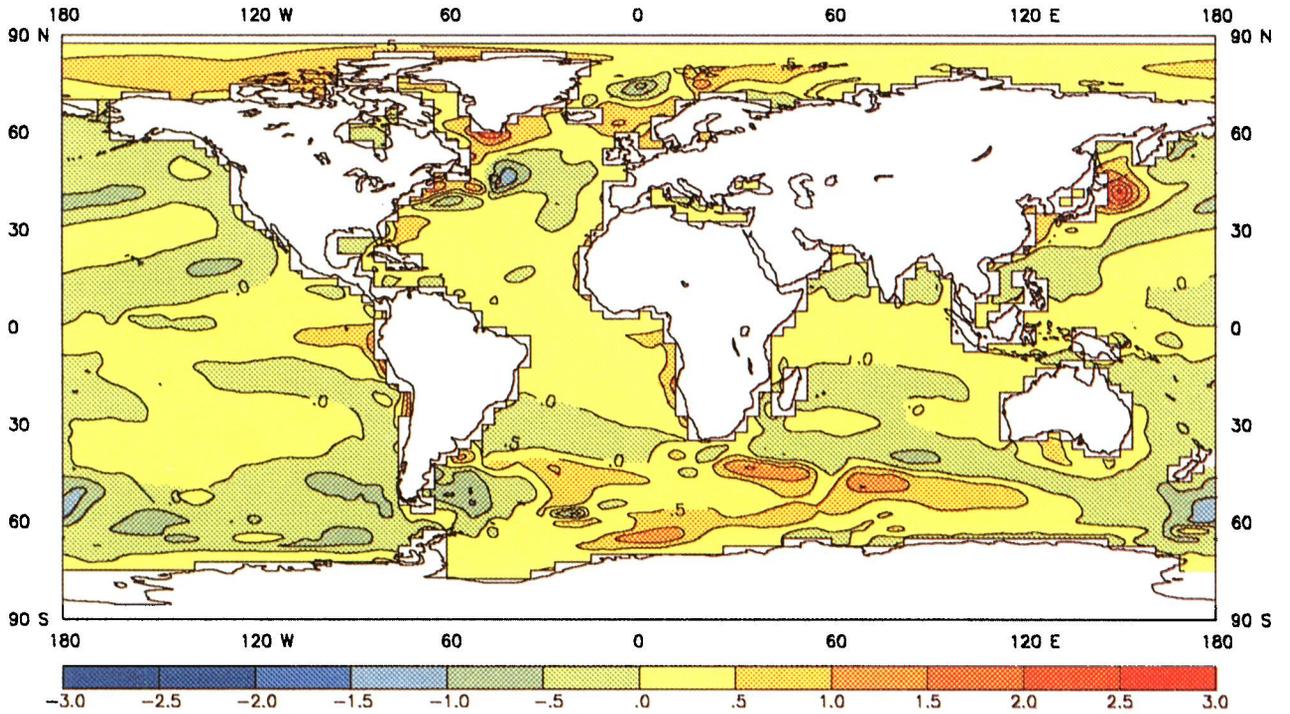
Figure 20. Five-year sea surface temperature anomaly (°C) produced by a coupled ocean–atmosphere run of the unified model.

Acknowledgements

The development of the unified model has been a cooperative project involving many staff from the Forecasting Research and Central Forecasting Divisions and from the Hadley Centre for Climate Prediction and Research. I wish to express my gratitude for their hard work and support in completing this project.

References

Corby, G.A., Gilchrist, A. and Rowntree, P.R., 1977: United Kingdom Meteorological Office five-level general circulation model. *Methods Comput Phys*, **17**, 67–110.

Cullen, M.J.P. and Davies, T., 1991: A conservative split-explicit integration scheme with fourth order horizontal advection. *Q J R Meteorol Soc*, **117**, 993–1002.

Cullen, M.J.P., Davies, T. and Mawson, M.H., 1991: Conservative finite difference schemes for a unified forecast/climate model. Meteorological Office, Unified Model Doc Paper no. 10. (Unpublished. Copy available from National Meteorological Library, Bracknell.)

Davies, H.C., 1976: A lateral boundary formulation for multi-level prediction models. *Q J R Meteorol Soc*, **102**, 405–418.

Gadd, A.J., 1978: A split-explicit integration scheme for numerical weather prediction. *Q J R Meteorol Soc*, **104**, 569–582.

—, 1985: The 15-level weather prediction model. *Meteorol Mag*, **114**, 222–226.

Gregory, D., 1990: Convection scheme. Meteorological Office, Unified Model Doc Paper no. 27. (Unpublished. Copy available from National Meteorological Library, Bracknell.)

Gregory, D. and Rowntree, P.R., 1991: A mass flux convection scheme with representation of cloud ensemble characteristics and stability dependent closure. *Mon Weather Rev*, **118**, 1483–1506.

Gregory, D. and Smith, R.N.B, 1990: Canopy, surface, and soil hydrology. Meteorological Office, Unified Model Doc Paper no. 25. (Unpublished. Copy available from National Meteorological Library, Bracknell.)

Ingram, W.J., 1990: Radiation. Meteorological Office, Unified Model Doc Paper no.23. (Unpublished. Copy available from National Meteorological Library, Bracknell.)

Jaeger, I., 1976: Monatskarten des Niederschlags für die Ganze Erde, *Ber Deutsch Wetterdienstes*, **18**, no. 139.

Milton, S.F., 1990: Practical extended-range forecasting using dynamical models. *Meteorol Mag*, **119**, 221–233.

Simmons, A.J. and Burridge, D.M., 1981: An energy and angular momentum and conserving finite difference scheme and hybrid coordinates. *Mon Weather Rev*, **109**, 758–766.

Smith, R.N.B., 1990: Subsurface, surface, and boundary layer processes. Meteorological Office, Unified Model Doc Paper no. 24. (Unpublished. Copy available from National Meteorological Library, Bracknell.)

Smith, R.N.B. and Gregory, D., 1990: Large-scale precipitation. Meteorological Office, Unified Model Doc Paper no. 26. (Unpublished. Copy available from National Meteorological Library, Bracknell.)

Unden, P., 1980: Changing the spherical grid for LFMs. LAM newsletter no.1, available from SMHI, Norrkoping, Sweden.

White, A.A. and Bromley, R.A., 1988: A new set of dynamical equations for use in numerical weather prediction and global climate models. Meteorological Office, Met O 13 Branch Memorandum. (Unpublished. Copy available from National Meteorological Library, Bracknell.)

Wilson, C.A., 1990: Vertical diffusion. Meteorological Office, Unified Model Doc. Paper no. 21. (Unpublished. Copy available from National Meteorological Library, Bracknell.)

Wilson, C.A. and Swinbank, R., 1990: Gravity wave drag. Meteorological office, Unified Model Doc. Paper no. 22. (Unpublished. Copy available from National Meteorological Library, Bracknell.)

Infrared imagery showing cloud evolution in a record(?) Atlantic low — 9/10 January 1993

T.D. Hewson
Joint Centre for Mesoscale Meteorology, Reading

It is probable that on 10 January 1993 a new low-pressure record* was set for a north Atlantic extratropical depression. Hand-drawn analyses from the Central Forecasting Office in Bracknell indicated surface pressure minima of 916 hPa at both 12 UTC and 18 UTC on the 10th. If the analyses are accurate it is likely that pressure fell below 916 hPa between 12 UTC and 18 UTC, to perhaps 914 or 915 hPa (at about 61° N, 15° W). This would beat the previous record* of 916 hPa, set on 15 December 1986 (see Burt (1987)). The largest 24-hour fall in central pressure in the depression was about 63 hPa, between 12 UTC on the 9th and 12 UTC on the 10th. The figure provides a pictorial record of the evolution of cloud and surface pressure during this exceptional development.

---

* Temporal and spatial gaps in the observational network make the precise definition of a low-pressure 'record' impossible.

At 12 UTC on the 9th the low was situated in a broad baroclinic zone oriented approximately east–west, as characterized by the broad cloud-band centred around 48° N. Evidence of the strong baroclinicity can be found in the UK Meteorological Office limited-area model (LAM) 900 hPa wet-bulb potential temperature pattern in the vicinity of the low; values ranged from 16 °C (just to the south) to about −6 °C (at 53° N, 40° W).

Between 12 UTC on the 9th and 00 UTC on the 10th relatively warm cloud to the north of the low emerges from underneath the main band of colder cloud, and cools considerably. This is the result of rapid large-scale ascent ahead of the developing low, which in turn is probably linked to warm-front frontogenesis. At the same time a relatively cloud-free zone appears to develop south of the low, suggesting large-scale compensating descent, which is probably linked to cold front frontolysis.
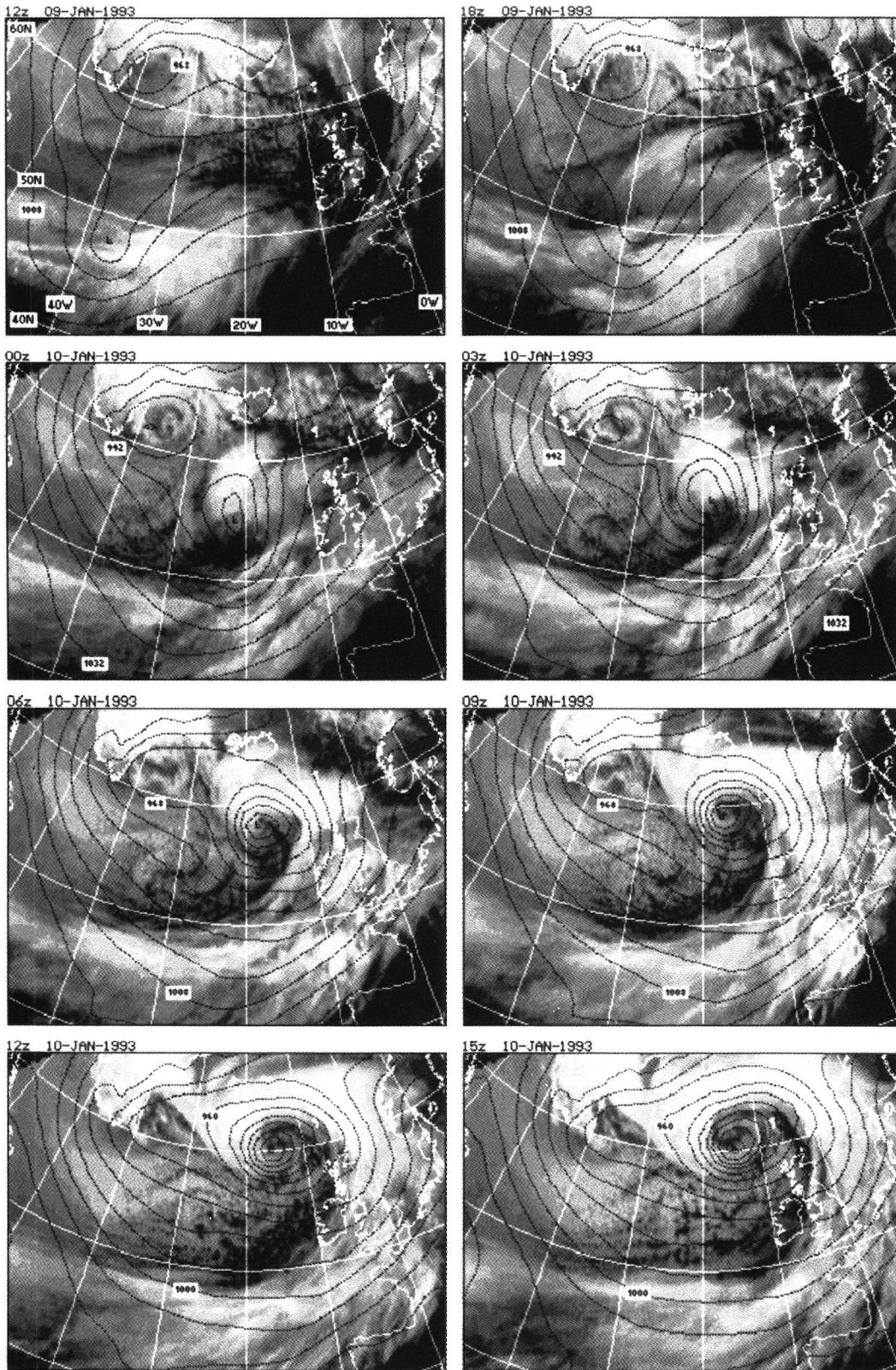
Meteosat infrared images for 9 and 10 January 1993, with concurrent surface isobars superimposed (contoured at 8 hPa intervals). The main centre of the low referred to in the text is marked by a small black dot, with 'L' alongside. Surface pressure was calculated using values of geopotential height of the 1000 hPa surface taken from the LAM. Isobars for 00, 06, 12 and 18 UTC are based on analyses whilst those for 03, 09 and 15 UTC are based on 3-hour forecasts. 'True' model surface pressure differs only slightly from that shown (generally by less than 2 hPa). Operational hand-analyses of surface pressure were also similar in this case (suggesting the position of 'L' is accurate to within 60 n mile).

During the 10th the low circulation intensifies considerably, causing the clear and cloudy zones to become intertwined, and resulting in the spiral cloud pattern apparent at 15 UTC.

Gyakum *et al.* (1992) have suggested that the maximum 24-hour pressure fall attained within a depression should be nearly proportional to the surface vorticity at the depression centre at the start of the 24-hour period in which that pressure fall occurs; such that a large surface vorticity will precede a large pressure fall. Extreme cases such as the depression of 9/10 January 1993 provide a good test of this hypothesis. In the 30 'rapidly developing' west Pacific cases examined by Gyakum *et al.* (occurring over a 9-year period), the geostrophic relative vorticity at the start of the 24-hour

period of maximum deepening ranged from 0.7×10^{-4} to 3.7×10^{-4} s^{-1}. The corresponding value for 12 UTC on 9 January 1993 (calculated using the same method) is 3.1×10^{-4} s^{-1}. Although this is close to the upper limit of the range for the Pacific cases it should be noted that in these the maximum 24-hour pressure fall was only 40 hPa, compared to 63 hPa observed here.

References

Burt, S.J., 1987: A new north Atlantic low pressure record. *Weather*, **42**, 53–56.

Gyakum, J.R., Roebber, P.J. and Bullock, T.A.,1992: The role of antecedent surface vorticity development as a conditioning process in explosive cyclone intensification. *Mon Weather Rev*, **120**, 1465–1489.

Thunderstorm activity in a developing cyclone — 4 January 1993

T.D. Hewson
Joint Centre for Mesoscale Meteorology, Reading

1. Introduction

Late on 5 January 1993 the oil tanker *Braer* capsized in gales and heavy seas just south of the Shetland Isles, an event which attracted much media coverage. The gales were associated with an Atlantic cyclone moving north-east towards the Norwegian sea. This cyclone had deepened by about 24 hPa on the 3rd, 14 hPa on the 4th and 1 hPa on the 5th. The figure relates principally to events on the 4th.

2. Observations

The infrared satellite image for 0300 UTC (top left) exhibits some features associated with explosive cyclogenesis, notably an extensive cloud head to the north and west of the low centre. What is unusual about this cloud head however is the isolated finger of cloud protruding from it around 49 °N, 32 °W. Animated hourly images show that this formed around 0100 UTC on the 4th, and persisted as a discernible feature for nearly 24 hours. During this period it moved north-east at 40–45 kn, remaining about 110 n mile north-east of the surface low centre, and undergoing only slight changes in orientation. On occasions during the animation small circular regions of colder cloud tops, tens of kilometres across, suddenly appear. In the subsequent 2–3 hours these regions expand and propagate westwards (relative to the system) and then south-westwards, apparently reinvigorating the cloud head. A blow-up of the eastern end of the finger of cloud at 0300 UTC indicates cloud-top temperatures above 0 °C, implying the cloud base there must be close to the sea surface.

The main figure shows that a large number of SFERIC* reports were associated with the finger of cloud. Light green and yellow symbols around 49° N represent lightning strikes between, respectively, 0230 UTC and 0250 UTC, and 0250 UTC and 0310 UTC (positional accuracy is about 10 n mile). The two black dots were plotted on this diagram to indicate end points of an axis of maximum lightning activity at the precise time of the Meteosat image (which is 0252 UTC for this part of the globe). This axis clearly propagates north-eastwards during the 4th, albeit with some fluctuations in the extent of lightning activity. Just before the activity finally died out it passed over ship Lima, at 57.2° N, 20.6° W. The 1900 UTC present weather observation from Lima was 'thunderstorm with rain' (code 95). This observation is also consistent with the 1700 UTC sounding from Lima, which indicated unstable air above 900 hPa.

3. Remarks

The finger of cloud on the Meteosat image clearly represents a persistent line of intense convective activity (hereafter referred to as LC). LC does not appear to be connected with either a cold front or a trough line; indeed surface charts for the 4th prepared at the Central Forecasting Office in Bracknell (not shown) depict an

---

* SFERIC reports come from the UK Meteorological Office arrival-time difference waveform-correlated lightning detection system, which operates in the VLF band.
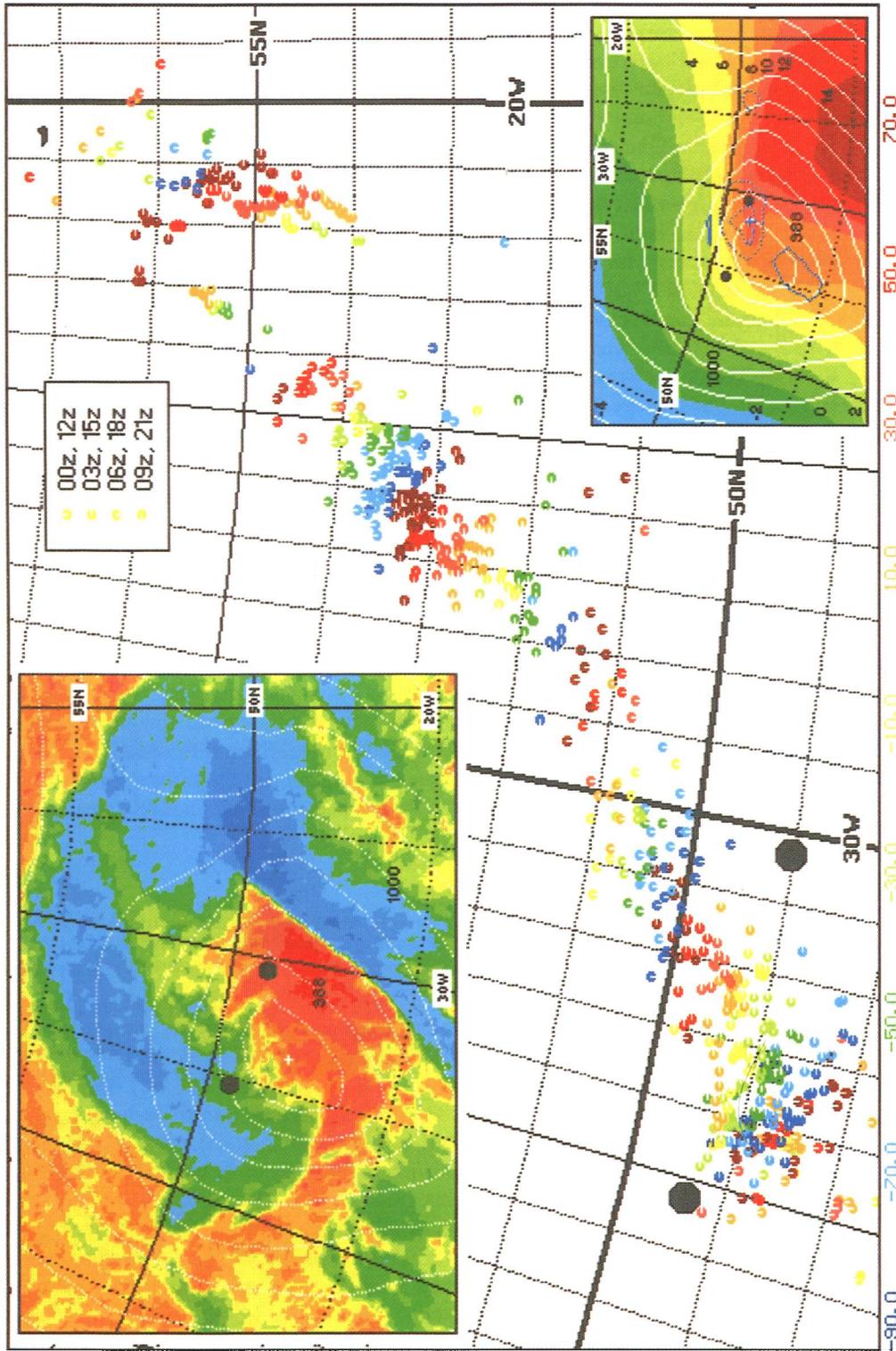
Main figure: all SFERIC reports registered in a given region of the north Atlantic during 24 hours ending 2230 UTC on 4 January 1993. During this period lightning activity transferred from the south-west of the domain to the north-east. The time of occurrence of each lightning strike is indicated by symbol shape and colour. Each symbol *shape* represents a 3-hour time-period centred on 00 UTC, 03 UTC, etc. (using 'clock' notation as shown in the small inset), whilst each *colour* represents a specific 20-minute period within the three hours (as shown by the scale at the foot of the diagram). For example the SFERIC at 49.7° N, 30.3° W was registered between −90 and −70 minutes relative to 0600 UTC: i.e. between 0430 and 0450 UTC.
Top left inset: Meteosat infrared image for 0300 UTC on 4 January 1993: each colour band relates to a 7 °C range of (approximate) cloud-top temperatures, the darkest blue being −63 to −56 °C. The 3-hour LAM surface pressure forecast for 0300 UTC is superimposed (contour interval 4 hPa); the cross indicates the low centre.
Bottom right inset: 3-hour LAM forecasts for 0300 UTC on 4 January of wet-bulb potential temperature at 900 hPa (colours, interval 2 °C), surface pressure (white contours; interval 4 hPa), and 2h (div(**Q**)) at 900 hPa (blue contours; at −150 × 10⁻¹⁶ (broken), −50 × 10⁻¹⁶ (broken) and +50 × 10⁻¹⁶ (solid) hPa⁻¹ s⁻³). The cross coincides with the minimum value of 2h (div(**Q**)) within the domain, i.e. 220 × 10⁻¹⁶ hPa⁻¹ s⁻³. Black dots collocate related features on the three figures (see text).

occluded front at its eastern end. The LAM 900 hPa wet-bulb potential temperature pattern (lower right inset) seems consistent with this frontal analysis, although it could be argued that it is in fact a warm front (see Monk (1992)). The average orientation of the analysed front on 4th (in the vicinity of LC) was about 070°, whilst that of LC itself was about 120°. One would not normally expect such features to be collocated. It would be valuable therefore to understand what mechanism gave rise to LC.

Diagnostic output from the UK Met. Office limited-area model (LAM) for the 4th, suggests that the eastern end of LC is consistently in a region of high relative humidity at 900 hPa (75–100%), and low static stability ($\delta\Theta$ = 5 °C between 1000 and 800 hPa); factors which are conducive to convective activity. In addition a large vertical wind shear was in evidence along LC (the vector wind difference between 1000 hPa and 500 hPa was initially about 70 kn, reducing to 40 kn late on the 4th). This is conducive to slantwise ascent. Thus vertical motion along LC probably comprised organized slantwise ascent, with embedded upright convective cells. Slantwise convection may also have been occurring, although it is unlikely that vertical velocities associated with this would be sufficient to generate lightning. Further analysis would be required to prove the atmosphere were unstable in a slantwise (as well as an upright) sense.

Convection over sea areas usually occurs in response to relatively high sea-surface temperatures, in polar air masses. LC, however, originates in a tropical air mass; sea surface temperatures would have to have been a few degrees higher to force the release of any instability. This suggests some other mechanism was triggering LC. A first candidate for this is dynamical forcing. Perhaps the simplest way to represent this forcing *at a particular pressure level* is by using the quantity 2h div($\mathbf{Q}$) where h is a (pressure dependent) constant, and $\mathbf{Q}$, the 'Q-vector', depends solely on potential temperature and geopotential height distributions at that level (see Hoskins and Pedder (1980)). In a simple quasi-geostrophic atmosphere vertical velocity is proportional to div($\mathbf{Q}$), negative div($\mathbf{Q}$) indicating ascent. The blue contours on the lower-right inset represent 2h div($\mathbf{Q}$) for 0300 UTC at 900 hPa·

The unusually low minimum value of -220×10^{-16} $hPa^{-1} s^{-3}$ (blue cross) coincides almost exactly with the right-hand end of LC. The two are also collocated at 06 UTC, 09 UTC and 18 UTC. If allowance is made for a probable LAM analysis error at 12 UTC, the two would also be collocated at 12 UTC and 15 UTC.

Thus it appears that LC represents the response to strong low-level quasi-geostrophic forcing of a moist, convectively unstable atmosphere containing large vertical wind shear. However, one caveat should be added. Div($\mathbf{Q}$) is evaluated using derivatives across length scales of 110 n mile, which is also the separation between surface low and LC. Coincidence may thus have caused LC and the minima in div($\mathbf{Q}$) to be collocated.

4. Comparison with other cases

Further imagery interpreted as depicting slantwise ascent can be found in Norris and Young (1991) and Shutts (1990). Both examples exhibit a gradual decrease in cloud-top temperature when moving from warm to cold (surface) air. Such a decrease is also apparent along LC in the image above. Shutts looked also at a successful model simulation of the storm of 16 October 1987. In the region where slantwise convection was believed to be taking place (at 06 UTC on the 15th) the vertical wind shear between 1000 hPa and 500 hPa was about 75 knots — again similar to that identified above.

In the two cited cases the lateral extent of the region of slantwise ascent, being over 300 n mile, is considerably greater than in this case. The cited cases also contain many 'striations' within this region, compared to the single finger apparent here. Such differences probably relate to subsequent deepening of the surface lows, which was explosive in the cited cases, but relatively small on 4 January 1993.

References

Hoskins, B.J. and Pedder, M.A., 1980: The diagnosis of middle latitude synoptic development. *Q J R Meteorol Soc*, **106**, 707–719.

Monk, G.A.; 1992: Synoptic and mesoscale analysis of intense mid-latitude cyclones. *Meteorol Mag*, **121**, 269–283.

Norris, J. and Young, M.V., 1991: Satellite photograph — 2 February 1991 at 1533 UTC. *Meteorol Mag*, **120**, 115–116.

Shutts, G.J., 1990: Dynamical aspects of the October storm 1987: A study of a successful fine-mesh simulation. *Q J R Meteorol Soc*, **116**, 1315–1347.

World weather news — January 1993

This is a monthly round-up of some of the more outstanding weather events the month, three preceding the cover month. If any of you, our readers, has first hand experience of any of the events mentioned below or its like (and survived!), I am sure all the other readers would be interested in the background to the event, how it was forecast and the local population warned.

These notes are based on information provided by the International Forecast Unit in the Central Forecasting Office of the Meteorological Office, Bracknell and press reports. Naturally they are heavily biased towards areas with a good cover of reliable surface observations. Places followed by bracketed numbers or letters in the text are identified on the accompanying map. Spellings are those used in The Times *Atlas.*

This month has been marked by exceptional violence in the North Atlantic and the tendency for all the tropical storms to affect land. Reports of these events have forced the exclusion of many reports that would otherwise have been included.
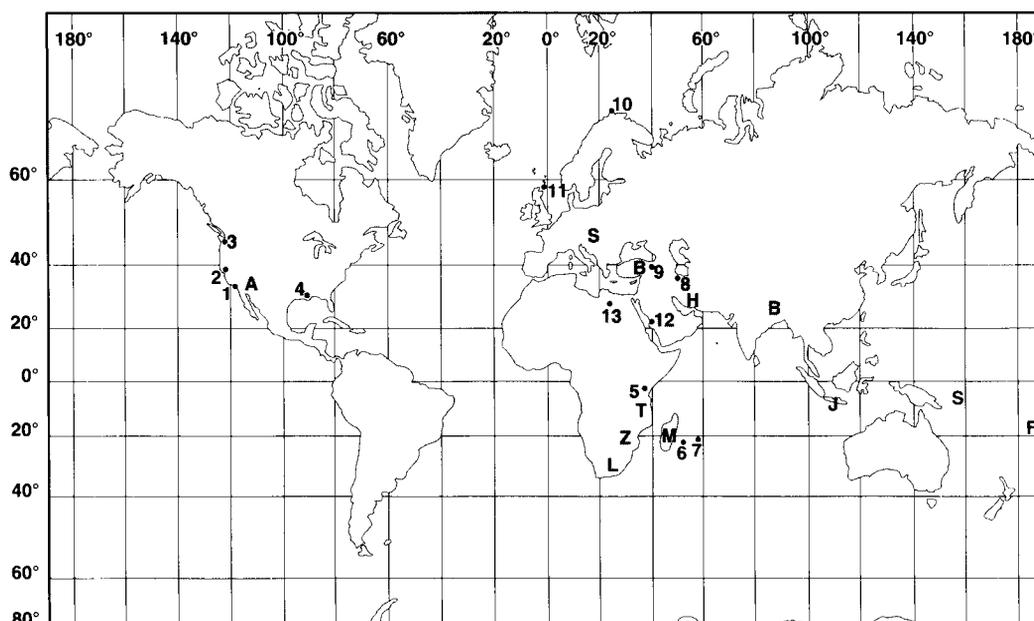
Location of places mentioned in text.

North America

Baja California had a week of rain to start the month and then on the 7th the rain became torrential with more than 60 mm in may places. Twenty-five died in Tijuana (1) where some city streets became muddy brown rivers. There was flooding as far north as San Diego County across the border in California, while in Mexicali nine were reported as having died of the cold. At this stage damage was estimated at $30m. On the 10th another storm threatened, and although most of Tijuana's streets were passable again, elsewhere there were mudslides and dams were close to overtopping. The threatened storm arrived on the 13th, and though the rain was not especially heavy, the saturated state of the ground lead to instant flooding with a further three drowned. Tijuana's drainage coped with this event and there were no deaths in the city though many were still unable to return to their homes.

Over the period 16th to 18th another severe rainstorm struck and the toll in Tijuana rose to 27. Seven died in southern California (a State of Emergency was declared in Orange and Santa Barbara counties). One death was reported in Arizona (A) where the floods were said to be the worst for ten years, with half the annual average rainfall in just ten days leading to the flooding of opencast mines and leaching pits. Rainfall in Los Angeles (2) reached 300 mm for the month with some major roads washed out and several 'million-dollar homes' were washed off their hillside foundations; rivers and reservoirs reached capacity, and in the nearby hills snow depths exceeded 3 m and some 25 buildings collapsed under the weight. At a submarine base in San Diego County a 'ten to fifteen foot wall of water' washed across the base overturning vehicles and stranding a helicopter. By the 17th San Diego's rainfall for January had reached 178 mm compared with the January average of 51 mm. By the 20th estimates were of $125m damage to insured property in the area and a death toll of 43.

The west coast was battered by further severe storms on the 20th with gales and heavy rain leading to five deaths from falling trees and power lines in Washington State. Floating bridges in Seattle Harbour (3) were

damaged and as far south as California gusts of 90 kn were reported. The costs run to about $175m.

Over the 19th/20th many places in the lower Mississippi had more than 100 mm (Lafayette is rumoured to have had 250 mm). By the 24th severe flooding along the lower reaches of the Mississippi led to the closing of lock gates near Baton Rouge (4) causing long delays to coastal barge traffic for the rest of the month.

Tropical and southern Africa

The 1st brought news that 37 were feared drowned when a bus was overturned by floodwater in southern Zimbabwe (Z). On the 7th Nairobi (5) had 52 mm, just over the average rainfall for all January.

Over the period 14/15th Morombe on the east of Madagascar (M) received 246 mm (but without any reports of thunder!): this comfortably exceeds the previous 24-hour total record of 199 mm. About this time cyclone 'Colina' developed and immediately started on the standard south-westerly course. On the 18th she started intensifying and recurving and the island of Réunion (6) battened down in preparation and all road traffic was banned. The storm struck on the 20th when central winds were at their maximum; on the island, mean wind speeds exceeded 40 kn and the maximum gust recorded was 90 kn with more than 100 mm of rain. Two died and twelve were missing afterwards; several dozen homes were destroyed and tens of thousands were cut of from fresh water and electricity; landslides and fallen trees blocked inland roads. Huge waves damaged the coast roads around St. Denis whose harbour was paralysed until the 22nd.

Later, on the 22nd, tropical storm 'Desilia' crossed the south of Madagascar and the January average rainfall of 185 mm was dropped in a day: immediately afterwards the temperature shot up to 37 °C. Nearer the end of the month, Mauritius (7) was at a precautionary standstill as cyclone 'Edwina' passed within 400 km on the 28th.

At the end of the month there were reports of two disasters: forty were killed and more missed after floods in north-west Tanzania (T) washed away homes and crops in Lesotho (L). The same rainfall event may have been responsible for an unseasonal flood which weakened a bridge near Darajani: at least 117 died when part of a Mombasa to Nairobi train fell into the river. One carriage is said to have been washed 1.5 km downstream. The bridge was built in 1898 but 'rarely repaired since'.

Australasia and Pacific

Cyclone 'Nina' passed through the Solomon Islands (S) on the 2nd killing three and rendering some 10 000 homeless (apparently on the islands of Rennel and Bellona nothing was left standing apart from a few buildings). The next day Cyclone 'Kina' struck the Fijian archipelago (F) killing 16, mostly in floods and high seas although 10 000 had been evacuated. The winds reached 100 kn and many were injured by flying debris. The west coast of Viti Levu was worst hit with two of the three principal bridges destroyed by the floods. Sava Airport was closed by flooding but Nandi, on Viti Levu, which had 66 mm of rain and gusts of 55 kn, was able to stay open. Although there was great damage to crops and live-stock, the sugar crop was already harvested. The cost was estimated at $150m.Tonga reported no damage, although there had been some concern.

Over the last few days of the month cyclone 'Lena' passed close to Flores (devastated by a tsunami late last year); heavy rains caused floods that killed five, and many boats were carried away by winds of 30 kn: in neighbouring East Jawa (J) and South Sulawesi fifteen were killed by floods. Damage was also done in eastern Jawa where many vessels were damaged around the port of Tanjung. Cyclone 'Lin' struck western Samoa on the last day of the month but nothing newsworthy seems to have resulted.

The weak tropical storm '14P' trundling over the north of Australia was producing winds of around 25 kn and, in a period of 60 hours up to the 29th, 330 mm of rain fell as temperatures dropped by 10° to 27 °C.

Asia

On the 8th and 9th there were reports of two tornadoes in north-east Bangladesh (B), these are said to have killed 76, injured about 3000, killed several hundred head of cattle and razed 15 000 bamboo huts. About the same time heavy snowstorms struck Iran causing chaos in Tehran (8) and closing many of the country's airports for some hours. Over the last few days of the month the Transcaucasian Highway was comprehensively blocked by avalanches near Vladikavkaz and Tbilisi. The death toll, in excess of fifty, including three at a research station on Mount Elbrus.

Europe, Arabia and North Africa

The month started very cold; in Turkey, Erzurum (9) had its all-time low temperature of −34.6 °C, resetting the record for the third time this winter. In Slovakia (S) more than 60% of the Danube was covered by ice, and all shipping movements were stopped because of the dangers. The 2nd and 3rd were the coldest days in central and southern Italy for seven years and there was a lot of snow, especially in Calabria (the 'toe') where the totals were the largest since the 1970s: Messina had its first snow for 25 years. Bari had a minimum of −2.1 °C and Cagliari −1 °C

Overnight on the 3rd/4th an intense, but not especially deep low, moved east near North Cape (10) and the Finmark area of Scandinavia experienced hurricane force winds of about 100 kn; these did several million pounds worth of damage but caused no fatalities even though a floating dock was destroyed. Early on the 5th the 90 000-tonne tanker *Braer* suffered a main engine failure and was subsequently driven ashore in the Shetlands, very close to the observing station of Sumburgh (03003) (11), by a 56 kn south-west wind with gusts to 74 kn. Waves

100

of 12 m prevented the crew of a tug from boarding the vessel to fix a towline. The tanker's crew had been airlifted to safety earlier when a previous grounding threatened. A major ecological disaster seemed imminent.

With pressure over south-east Europe over 1040 hPa at this time there was plenty of scope for 'bora' and 'mistral' type winds: next day two more ships met trouble, but in the Mediterranean this time. The 4000-tonne *Coty 1* with a cargo of cement encountered a force 10 with 12 m waves near the island of Kithira. After a temporary engine failure the ship took a severe list and the crew abandoned ship but many were lost when the lifeboats were swamped. The *Marineta* was carrying kaolin when she took on water and grounded in heavy seas whipped up by a force 7 near Crotone on the 'heel' of Italy. Strong westerly winds on the 6th brought blizzards to the north of Saudi Arabia though Jiddah (12) still managed 34 °C (beating the January record). Further west, Siwa (13) in north-east Egypt had 13 mm of rain; not a big deal until compared with the January record of 4 mm! Cairo had its coldest day of the winter so far on the 7th when the maximum was only 12 °C.

Back north, on the 9th the 689-tonne *Stavfjord*'s cargo of fertilizer, detonators and 200 tonnes of dynamite shifted. During the attempted salvage the tow line broke three times in hurricane force winds and mountainous sea. The crew were airlifted to safety, but two days later the cargo exploded off Skjervøy, north Norway. A different kind of explosion now occurred: in the early hours of the 10th explosive cyclogenesis occurred north-west of the British Isles. Between 0400 and 0500 UTC pressure fell 10 hPa at OWS *Cumulus* and as the low deepened to 916 hPa the ship was battered by winds reaching 105 kn with 10 m waves. At the time of writing this, in April, it still seems that the resulting tumultuous seas dispersed the entire cargo of oil from the *Braer*, which unsurprisingly broke up. Over the period of 9th to 11th the Stratfjord oilfield off Norway was virtually closed down because waves of up to 17 m prevented any tankers approaching to load the oil normally stored in the hollow legs of the platforms. Production was restarted on the 14th when waves were only 4.2 m. Tankers were again prevented from approaching on the 16th and 17th and, later, on the 21st.

The storms of the first half of the month were so severe, that on some of the islands of northern Britain, archaeological sites have been destroyed but others revealed.

The heavy rain of the 11th/12th in Belgium caused the worst flooding there since 1926 when both the Meuse and the Ourthe rivers burst their banks. On the 13th, a small but intense low raced east-north-east across southern Britain, winds gusted to 85 kn in the south-west and pressure changed 15 hPa (both down and up) in three hours. It then moved on to give the southern North Sea and Baltic wild weather. Winds of 90 kn in north Germany uprooted trees, traffic lights and removed roofs. Heavy rain raised the Elbe to 5 m above normal, closing

the centre of Lübeck to traffic: in Hamburg a State of Emergency was declared for a few hours during the night. Copenhagen port was a dangerous place as empty containers were shifted by the wind and a coal crane was blown over; 75 cars were 'sandblasted' by small debris. In Lithuania and Latvia the storm was the worst since 1967 with winds speeds of over 65 kn: six were killed, vessels broke their moorings and were blown out to sea, 21 railway stations lost their electricity supplies as 7800 sub-stations failed, depriving the grid of 350 MW. At Vilnius airport a Boeing 737 was blown off the runway onto rough ground just after landing, but there were no casualties. In Poland the storm brought a thaw and the pressure of ice caused the collapse of the longest (about 1400 m) wooden bridge in Europe — over the Vistula at Wyszogrod north of Warsaw. The 3000-tonne Polish ferry *Jan Heweliusz* sailed from Sweden into the storm and 52 were drowned when she capsized, nine survivors were rescued from the mountainous, icy seas. There is a theory that despite the winds of nearly 90 kn the enclosed bridge insulated the master from the storm to the extent that he did not realize how violent conditions were.

On the 17th a larger, very intense, low moved north-east just off the Hebrides, severe gales and heavy rain brought a rapid thaw of deep snow to Scotland. At Kirkwall in Orkney the hourly mean speed reached 66 kn with a gust to 94 kn. Other notable gusts were 91 kn on Fair Isle and 130 kn on the summit of Cairn Gorm. During this period Aviemore's rainfall total reached 209 mm for a new January record, and the 50 cm of snow lying on the 14th melted to a mere 1 cm by the 19th. As a result flooding was widespread and the River Tay rose to 4.25 m above normal. RAF helicopters rescued twenty from flooded houses and the Army used inflatable dinghies to evacuate a housing estate. Most north–south road and rail links were cut and the cost was later estimated at about £10m.

In contrast to all the excitement in the north, southern Europe was stagnant under high pressure and cars were banned from central Athens on the 19th because of dangerous levels of smog. On the eastern side of the high severe cold weather swept into the 'Near East' around the 18th. In Bayburt province (B), north-east Turkey, an avalanche killed 58 and injured 25 when 43 out of the 96 houses in one village were overwhelmed after 2 m of snow fell in a blizzard. Later, widespread flooding was reported in south-east Iran in Hormozgan (H) and some flooding in Jiddah. The recent rains in this latter area have created favourable breeding conditions for the desert locust and swarms have been reported along the Red Sea coasts.

Wild weather continued in higher latitudes when a low of about 952 hPa passed close to Scotland, and Glasgow had a wind of 76 kn. This pales to insignificance compared with the (new record?) speed of 147 kn on Cairn Gorm. The last low in this viscious series tracked a little further south with north-westerly winds in its rear: on the 24th the Baltic coast of Poland was battered by severe

gales that caused widespread damage and closed ports. Coastal communities were put on standby for evacuation as the storm surge flooded Kaliningrad and surrounding areas.

The storms in the first half of the month did about £155m worth of damage in the United Kingdom in addition to about £15m in the Perthshire floods.

Stop Press — *Africa*

The following is part of a news release from the World Climate Programme of WMO.

'In Kenya and in neighbouring East African states, January is perceived as a dry month; the short rains are over by mid or late December and the hot dry north-easterly monsoon banishes the rain clouds. They would not be expected to return before late March. January 1993, in Kenya, was not hot and dry. It was cool and very wet. Rainfall was unprecedented, unexpected and disastrous.'

More details next month.

January tropical storms

This is a list of tropical storms, cyclones, typhoons and hurricanes active during January 1993. The dates are those of first detection and date of falling out of the category through dissipation or becoming extratropical. The last column gives the maximum sustained wind in the storm during this month. The maps show 0000 UTC positions: for these I must thank Julian Heming and Susan Coulter of the Data Monitoring group of the Central Forecasting Office.

No	Name	Basin	Start	End	Max. (kn)
1	Colina	SWI	14/01	21/01	105
2	Dessilia	SWI	20/01	23/01	35
3	Edwina	SWI	20/01	29/01	120
4	Nina	AUS	23/12	03/01	75
5	Kina	AUS	27/12	03/01	100 in January
6	Lena	AUS	24/01	29/01	55
7	14P	AUS	26/01	27/01	35
8	Lin	AUS	31/01	—	55

Basin code: SWI — west Indian Ocean (south); AUS — Australasia.

Australasia

West Indian Ocean
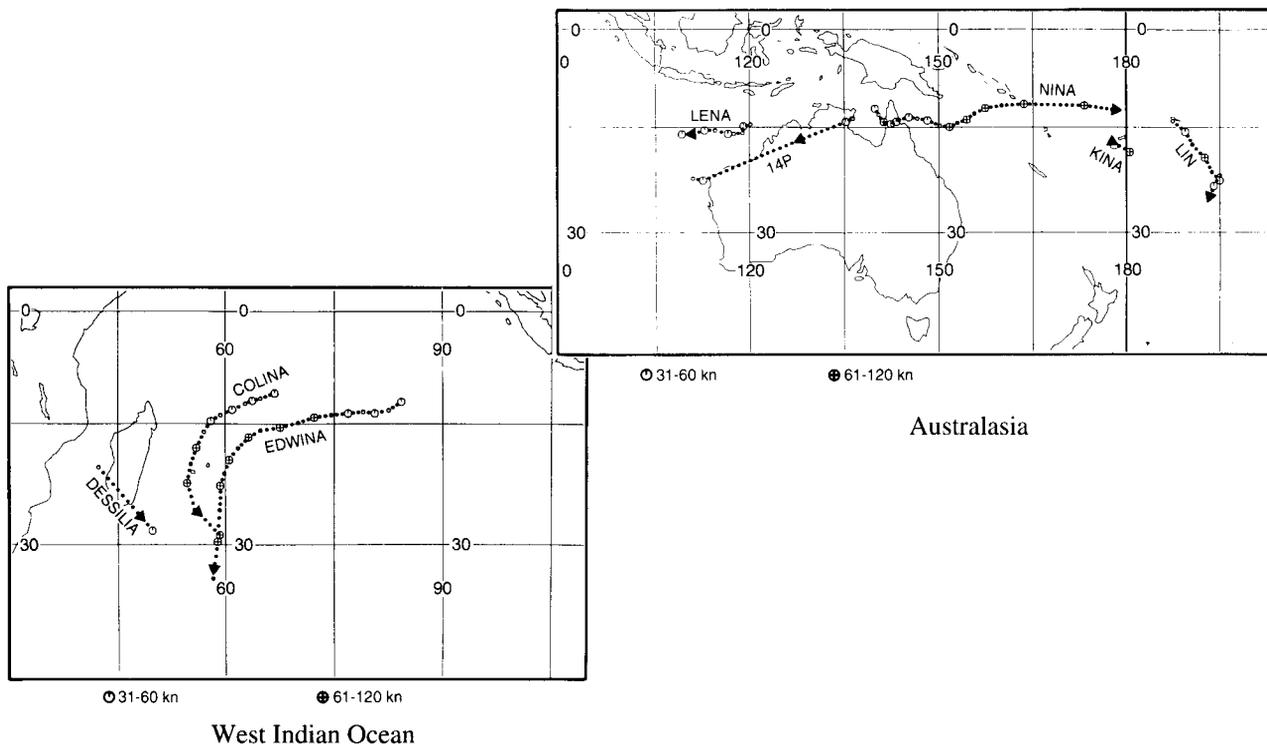
Awards

Meteorological Office scientists win international award

On Tuesday 23 February 1993 four Meteorological Office scientists were presented with the prestigious Professor Dr Vilho Vaisala Award by the Secretary-General of the World Meteorological Organization (WMO), Professor G.O.P. Obasi.

David Griggs, Wynn Jones, Martin Ouldridge and Bill Sparks won the Award for their intercomparison of visibility instruments carried out on behalf of the WMO during 1988–89.

Their paper not only described the conduct and results of the intercomparison but also recommended accuracy standards and ways to use the instruments operationally. This information will be of considerable value to meteorologists around the world in choosing the right visibility instruments for their individual needs and gaining maximum benefit from the data. It will also be useful to motorway and airport authorities and others who need to measure the visibility for their various applications.

The winners of the Award worked within the Observations Division of the Met. Office to produce the paper, entitled 'The first WMO intercomparison of visibility measurements'. Wynn Jones was the Project Leader, David Griggs was Technical Manager and Bill

Left to right. Martin Ouldridge, Professor Obasi, David Griggs, Richard Pettifer (Vaisala UK) and Bill Sparks. Wynn Jones was unable to attend the ceremony.

Sparks and Martin Ouldridge were in charge of data processing and analysis.

The work was carried out as part of the continuing survey of atmospheric sensors and meteorological observing systems which is one of the Office's functions as the National Meteorological Service. The results of such studies are available to all.

This is the seventh presentation of the Award — and the fourth time it has been won by staff members of the Office. The Award consists of a diploma, a medal and a cheque for $2500 each.

Professor Obasi, in presenting the Award, said 'This research work is a valuable contribution to the work of the World Meteorological Organization (WMO) and to the advancement of instrumentation. I congratulate the winners and convey to them the warm congratulations of the President of WMO, the Members of the Executive Council and indeed all Members of the WMO.'

Meteorological Office wins six major TV awards

The Met. Office won six awards at the International TV Weather Forecasters Festival ending on Friday 12 February in Paris.

Siân Lloyd from the Meteorological Office's International Weather Productions (IWP) ITV National Weather was equal first in the Prix des Preséntateurs, being chosen by all the other presenters from 55 entries from 40 countries. Bill Giles for the BBC Weather Centre and BBC World Service Television was third.

In the Prix des Scientifiques, awarded for scientific content, the BBC came second and IWP fourth.

In the most prestigious award, the Trophee du Festival, IWP was voted second, and the BBC World Service TV came third.

The winner of the Trophée du Festival, Danny Roup of Israel, told the audience that he owed his award to IWP for all the help, training and information they had given him over the last two years. This accolade was reinforced by other presenters in Germany and Switzerland. IWP has been developing international business during the year through a range of services, including TV2 in Norway provided in collaboration with the Norwegian Met. Service.

IWP has made several changes to the ITV National Weather during the course of the last year, modifying design, animation, map colours and cloud shapes in response to market research. IWP has also been working closely with the Met. Office's network of Weather Centres to develop a wide range of new services in the ITN regions, including LWT, Carlton, and HTV.

Siân Lloyd has been working for IWP as a presenter for ITV National Weather since 1990. Before then she worked for BBC Wales, Channel 4 Wales and the Mid Wales Development Board. Siân has a background of

languages and journalism, and has been trained in meteorology at the formal course in Meteorology for Weather Presenters at the Met. Office College near Reading.

Bill Giles has been head of the BBC Television forecasting team since 1983. He joined the Met. Office in 1957 and has been forecasting for radio and television most of the time since 1972.

The BBC Weather Centre, combining BBC and Met. Office skills and resources, produces the BBC national and international forecasts. World Service TV includes weather information for all over the world, with detailed inserts for Europe, Asia and Africa.

Correspondence

Hoar-frost deposition

The letter from N. Gait and T. Hewson (*Meteorol Mag*, **121**, 268) suggested that when hoar frost is localized, the road hazard may be less obvious to motorists, and so more dangerous through being intermittent and unexpected. If this logic is accepted, the same would apply to the dampness caused by road salting. Although its dampening effect is usually extensive and persistent, it is not consistently so. Depending on humidity and other factors, there are often periods during the afternoon and early evening when the salt dries temporarily. During these periods, occasional damp patches remain where the sun has not reached. Presumably these patches could be regarded as disproportionately dangerous because motorists may not be expecting them.

By the same logic, it could be argued that icy patches left on unsalted roads are made more dangerous by the salting of main roads (because the residual ice will be more of a surprise to motorists). Many journeys begin or end on unsalted surfaces: it is not practical to salt every minor road and side street, and local authorities do not attempt to do so.

I suggest, however, that such arguments should not be overemphasized. In practice, whenever there is serious and widespread ice, there is a spate of ice-related accidents. The more ice there is, the more ice-related accidents there are. The obviousness of the hazard does not seem to make up for its extensiveness. Similarly when roads are generally wet, from salt or any other cause, there are more accidents than when they are mainly dry, despite the occasional damp patch.

None of this detracts from the potential usefulness of the original paper (*Meteorol Mag*, **121**, 1–21). It showed that the hazard from hoar frost deposition is particularly associated with circumstances such as short day length, a shallow layer of moist air, and a definite but gentle breeze accompanying clear skies, especially after successive clear nights. These findings could be very useful in preparing forecasts for highway authorities. But no practical benefit will ensue unless forecasters are prepared to adjust their road-ice forecasts in such a way as to advise against salting on some occasions when it might otherwise have taken place.

Experience of personal observation during the 1992/3 winter was that the surfaces of unsalted side streets were only rarely (and briefly) affected by ice from hoar-frost or any other mechanism. The number of occasions on which main and intermediate roads were salted was much greater. In addition there were long periods during which roads were not subject to fresh salting but were still affected by residual salt from previous operations (in the absence of rain since the last frost). These observations relate mainly to the Home Counties around the northern edge of London. It seems that in practice, significant ice problems on untreated roads are much rarer than would be expected on the basis of road surface temperature (RST) below dew-point (when below 0 °C).

R. Mansell

8 Curthwaite Gardens
Enfield
Middlesex
EN2 7LN

Dear Sir,
Congratulations on your new feature on world weather in the January issue of the *Meteorological Magazine*.

These days meteorologists have fewer opportunities of experience in tropical and sub-tropical regions than people of my generation had. I spent nine years between 1943 and 1963 on three overseas tours, covering southeast Asia, the Middle East and the Mediterranean, so that references in your first article to weather events in places familiar to me were especially interesting — and nostalgic! For most younger meteorologists their experience of weather overseas is usually limited to short holidays!

It is good for all of us to be aware of the international nature of weather. The destructiveness and economic cost of some weather events overseas put weather happenings in the UK into perspective.

R. Murray
(Met. Office 1939–1977)

Wokingham
Berkshire

GUIDE TO AUTHORS

Content

Articles on all aspects of meteorology are welcomed, particularly those which describe results of research in applied meteorology or the development of practical forecasting techniques.

Preparation and submission of articles

Articles, which must be in English, should be typed, double-spaced with wide margins, on one side only of A4-size paper. Tables, references and figure captions should be typed separately. Spelling should conform to the preferred spelling in the *Concise Oxford Dictionary* (latest edition). Articles prepared on floppy disk (IBM-compatible or Apple Macintosh) can be labour-saving, but only a print-out should be submitted in the first instance.

References should be made using the Harvard system (author/date) and full details should be given at the end of the text. If a document is unpublished, details must be given of the library where it may be seen. Documents which are not available to enquirers must not be referred to, except by 'personal communication'.

Tables should be numbered consecutively using roman numerals and provided with headings.

Mathematical notation should be written with extreme care. Particular care should be taken to differentiate between Greek letters and Roman letters for which they could be mistaken. Double subscripts and superscripts should be avoided, as they are difficult to typeset and read. Notation should be kept as simple as possible. Guidance is given in BS1991: Part 1:1976 and *Quantities, Units and Symbols* published by the Royal Society. SI units, or units approved by the World Meteorological Organization, should be used.

Articles for publication and all other communications for the Editor should be addressed to: The Editor, Meteorological Magazine, Meteorological Office Room 709, London Road, Bracknell, Berkshire RG12 2SZ.

Illustrations

Diagrams must be drawn clearly, preferably in ink, and should not contain any unnecessary or irrelevant details Explanatory text should not appear on the diagram itself but in the caption. Captions should be typed on a separate sheet of paper and should, as far as possible, explain the meanings of the diagrams without the reader having to refer to the text. The sequential numbering should correspond with the sequential referrals in the text.

Sharp monochrome photographs on glossy paper are preferred; colour prints are acceptable but the use of colour is at the Editor's discretion.

Copyright

Authors should identify the holder of the copyright for their work when they first submit contributions.

Free copies

Three free copies of the magazine (one for a book review) are provided for authors of articles published in it. Separate offprints for each article are not provided.

Contents